

DESIGN AND MECHANICAL BEHAVIOR OF THE MD SERIES OF BONE
DOWELS

By

JOHN R. BIANCHI

A DISSERTATION PRESENTED TO THE GRADUATE SCHOOL
OF THE UNIVERSITY OF FLORIDA IN PARTIAL FULFILLMENT
OF THE REQUIREMENTS FOR THE DEGREE OF
DOCTOR OF PHILOSOPHY

UNIVERSITY OF FLORIDA

1999

This dissertation is dedicated to Dominick and Jean Bianchi, who raised me to fill the space between my ears; to my brother, Michael, who has somehow managed a great excuse in NOT going to another graduation; and to my wife, Laurie, who has managed to find herself in another. One of the most unselfish acts one human may do for the other is to share the gift of organ and tissue donation. This research is dedicated to the memory of the donors and their families. For if it had not been for them, this research would never have been possible.

ACKNOWLEDGMENTS

I wish to thank Dr. Chester E. Sutterlin III, MD, for teaching me about spinal surgery and how to apply my knowledge of engineering to its practice. I thank Jamie Grooms and Regeneration Technologies Inc for financial support of this project and having the stamina to ensure that it was carried out. I am grateful to John J. Mecholsky, Jr. for his patience and judgement, and Christopher Batich for encouraging me to begin my studies at UF. I would like to thank my Doctoral committee, Anthony Brennan, Edward Walsh, David Greenspan, and Andrew Rapoff for ensuring that this research was carried out to the highest of standards. I am thankful to C.Randal Mills for his intellectual conversations, and James E. Keesling Jr, an Engineer who crossed the line and became a Statistician, assisting with many of the statistical analysis. I would to thank Chris Glymph for setting this research to practice, Kevin Carter for his most valuable technical assistance, Kevin Ross for helping out with the mechanical testing, and Sanna Martinez-Saare for her artistic sketches. But most of all I would like to thank and acknowledge my wife for her patience, pep talks, comic relief, and love.

I would like to thank many of my family and friends who insured that I had a good time including the founding members of the Thundering Amoeba Investment Club: Matt Corrigan, Mike Rickey, Doug Mullin, Dan Garlington, Will Lyons, and Mike Lyons.

TABLE OF CONTENTS

	<u>page</u>
ACKNOWLEDGMENTS	iii
LIST OF TABLES	vii
LIST OF FIGURES	ix
INTRODUCTION	1
REVIEW OF THE LITERATURE	5
The Function and Anatomy of Bone.....	5
Mechanics of Bone	7
Historical Development of Bone as a Transplantable Material.....	14
Indications for Spine Surgery	19
Surgery of the Spine.....	20
Spinal Mechanics	20
Mechanics of Spine Fusion.....	21
Biology of Spine Fusion	21
Synthetic Implants Used for Spinal Fusion	22
Bone Grafts Utilized in Spine Surgery	23
Interbody Autografts or Allografts for Spine Surgery	23
Structural Properties of Allograft Interbodies for Spinal Fusion.....	38
Alternative Materials to Bone.....	39
Alternatives to Spinal Fusion.....	40
Summary	40
LOCAL STRESS FIELD.....	42
Introduction.....	42
Materials and Methods.....	42
Results.....	46
Hertzian Contact Between Concentric Cylinders	46
<i>In-Vivo</i> Loading Conditions.....	46
Discussion	49
Conclusions.....	51
NORMALIZED STRENGTH	52
Structural Characteristics of Bone	52

Structural Characteristics of Bone Dowels	54
Theoretical Stress Analysis.....	55
Modes of Loading	55
Materials and Methods.....	56
Specimen Preparation	56
Mechanical Testing.....	56
Physical Measurements.....	58
Data Analysis.....	58
Normalized Strength	59
Results.....	60
Failure Load of MD-II Bone Dowels.....	60
Failure Loads of MD-II Dowels as a Function of Diameter	61
Failure Load as a Function of Dimensions	61
Failure Loads as a Function of Density, Hardness, or Ultrasonic Velocity.....	67
Analyzing the Data by Multivariable Regression Analysis	70
Applicability to the Bone Dowels.....	75
Conclusions.....	75
 BIOMECHANICAL QUALITY CONTROL PROCEDURE.....	 77
Introduction.....	77
Materials and Methods.....	77
Normalized Strength of Bone Dowels	77
Acceptable Quality Criteria	78
Design Loads on the Dowels	78
Probability of Survival.....	78
Weibull Approach Applied to the Bone Dowels	79
Validation.....	80
Specimen Preparation	81
Sample Size.....	81
Nondestructive and Destructive Analysis.....	81
Results.....	82
Weibull Modulus, Intercept and Threshold Load	82
Validation Results.....	85
Results in Manufacturing Since Implementation of NDE at RTI.....	85
Conclusions.....	88
 PROCESSING AND DONOR DEMOGRAPHICS OF CORTICAL BONE.....	 89
Introduction.....	89
Materials and Methods.....	90
Specimen Preparation	90
Experimental Design.....	91
Treatment Groups	92
Physical and Mechanical Testing.....	94
Results.....	97
Discussion.....	100

Conclusions.....	106
DONOR DEMOGRAPHICS, PROCESSING, AND DESIGN OF THE MD SERIES OF BONE DOWELS	108
Introduction.....	108
Materials and Methods.....	108
Specimen Preparation	108
Donor Attributes	109
Processing Parameters	109
Dowel Design.....	110
Experimental Design.....	110
Mechanical Testing.....	111
Normalized Strength	111
Statistical Analysis.....	111
Results and Discussion	112
Donor Demographics	112
Processing Parameters	114
Design	115
Conclusions.....	116
SUMMARY	117
REFERENCES	120
APPENDIX RAW DATA, REGRESSION, AND WEIBULL ANALYSIS	132
BIOGRAPHICAL SKETCH	139

LIST OF TABLES

<u>Table</u>	<u>page</u>
2-1 Ultimate strength of human cortical and cancellous bone.....	9
2-2 Elastic constants for human cortical bone	9
2-3 Axial load bearing capacity of different vertebral levels	20
2-4 In vivo loading on the human spine.....	21
2-5 Load bearing capacity of various interbodies.....	38
4-1 Best regression subsets	72
4-2 Regression coefficients for various size dowels.....	72
5-1 Minimum sample size for validation	81
5-2 Possible Outcomes for validation	82
5-3 Weibull analysis results for various dowels	83
5-4 Validation actual outcomes	85
6-1 Axial compression treatment groups	93
6-2 Shear treatment groups	93
6-3 Diametral compression treatment groups.....	93
6-4 Density of each compression group prior to treatment.....	97
6-5 Ultimate compressive strength of each treatment group	97
6-6 Density of each shear group prior to treatment	98
6-7 Ultimate shear strength of each treatment group.....	98
6-8 Density of each transverse tension group prior to treatment.....	98

6-9 Ultimate transverse tensile strength of each treatment group.....	99
7-1 Bone dowel treatment groups	110
7-2 Variation of strength of 16mm MD-2 due to anatomic origin	112
7-3 Variation of strength of 18mm MD-2 due to anatomic origin	112
7-4 Variation of strength of 16mm MD-III as a function of donor age.....	113
7-5 Variation of strength of 16mm MD-II as a function of donor age	113
7-6 Variation of strength of 18mm MD-II as a function of donor age	114
7-7 Variation of strength of 20mm MD-II as a function of donor age	114
7-8 Variation of strength of 16mm MD-II due to processing.....	115
7-9 Variation in strength between 16mm MD-II and MD-III dowels	116
7-10 Variation in strength between 18mm MD-II and MD-IV dowels	116

LIST OF FIGURES

<u>Figure</u>	<u>page</u>
1-1 Sketch of typical MD-II bone dowel	4
2-1 Cloward dowel.....	27
2-2 Crock Dowel.....	27
2-3 Vich threaded cancellous dowel	28
2-4 MD-II and MD-III cortical bone dowels	28
2-5 Smith-Robinson iliac crest graft	32
2-6 Bailey-Bagley iliac crest graft	32
2-7 Tangent™ cortical wedge.....	33
2-8 Cortical ring from long bone	35
2-9 SR™ graft.....	35
2-10 Vertigraft™	36
2-11 FRA-Spacer™	36
2-12 ALIF™	37
3-1 Test Jig for Moiré Loading.....	45
3-2 Hertzian contact stress V-field	47
3-3 Hertzian contact stress U-field	47
3-4 <i>In-vivo</i> loading V-field	48
3-5 <i>In-vivo</i> loading U-field	48
3-6 Typical fracture patterns observed in bone dowels under axial compression	50

4-1 Cross-section of human femur.....	53
4-2 Typical production dowels	54
4-3 Dowel under axial compression	57
4-4 Histogram of failure loads	63
4-5 Average failure loads of different size MD-II dowels.....	64
4-6 Histogram of failure loads of 16 and 20mm MD-2 dowels.....	65
4-7 Failure load as a function of endwall thickness.....	66
4-8 Failure load of 16mm MD-II as a function of density.....	68
4-9 Failure load of 18mm MD-II as a function of density.....	68
4-10 Failure load of 16mm MD-II as a function of ultrasonic velocity in cortical ring	69
4-11 Failure load of 16mm MD-II as a function of hardness of cortical bone	69
4-12 Multiple regression analysis of 16mm MD-II bone dowels.....	73
4-13 Multiple regression analysis of 18mm MD-II bone dowels.....	73
4-14 Multiple regression analysis of 20mm MD-II bone dowels.....	74
5-1 Probability plots of 16 and 18mm MD-2 dowels	84
6-1 Shear Test Fixture.....	95
6-2 Test configuration for axial and diametral compression	96
A-1 Determination of Weibull modulus for 16mm MD-2.....	138

Abstract of Dissertation Presented to the Graduate School
Of the University of Florida in Partial Fulfillment of the
Requirements for the Degree of Doctor of Philosophy

DESIGN AND MECHANICAL BEHAVIOR OF THE MD SERIES OF BONE
DOWELS

By

John R. Bianchi

December 1999

Chairman: John J. Mecholsky, Jr.

Major Department: Materials Science and Engineering

Allograft bone dowels, developed at the University of Florida Tissue Bank, Inc (UFTB) and Regeneration Technologies, Inc (RTI), offer an alternative to the more conventional metallic and other synthetic dowels for spinal fusions. These dowels are machined from the long bone of human donor tissue. They are an advance over current implants because they possess the precise dimensional characteristics that are typical of metallic or other synthetic implants, are composed of mostly cortical bone, do not cause additional donor site morbidity associated with autografts, yet they retain the advantageous osteogenic characteristics of allografts and autografts.

Allograft and autograft tissues have a well-established history in spinal fusions. However, postoperative failures are commonly reported. These failures are due to the variations in geometric, material, and mechanical properties of the implants. In addition,

little research effort has been placed on insuring that these types of implants have at least a minimum level of load bearing capacity.

The results of this research developed a novel method, based on statistical procedures and fracture mechanisms, that defines the strength of the MD-series of bone dowels and uses this technique to establish a nondestructive mechanical quality control procedure. In addition, the influence of donor characteristics such as age, and sex on the strength of the dowels was established. The role of different tissue banking processing steps on the strength of machined tissue was identified, as well as differences in strength among different dowel designs determined.

CHAPTER 1 INTRODUCTION

Allograft bone dowels, developed at the University of Florida Tissue Bank, Inc (UFTB) and Regeneration Technologies, Inc. (RTI), offer an alternative to the more conventional metallic and other synthetic dowels for spinal fusions. The MD-series (machined dowel) of dowels were developed as an intervertebral spacer for spinal fusion. The dowels are machined from the long bone of human donor tissue. They are an advance over current implants because they possess the precise dimensional characteristics that are typical of metallic or other synthetic implants, are composed of mostly cortical bone, do not cause additional donor site morbidity associated with autografts, yet they retain the advantageous osteogenic characteristics of allografts and autografts.

Bone dowels are manufactured from the long bones of humans. Generally, a dowel may be machined from a male or female donor between the ages of 15-70 years. Typically, the dowels are obtained from the femur, tibia, and humerus. In addition, if the anatomy of the bone will allow for machining of the implant, dowels may be obtained from the radius and ulna.

Dowels are cut perpendicular to the long axis of the bone within the diaphysis. Generally, the angle of the cut is made which will yield the dowel with the best dimensional characteristics. Typically, this is an anterior-to-posterior cut. The last machining step is to place threads on the outside surfaces of the dowel. The threads serve

two primary purposes. They allow for ease of insertion and prevent the graft from backing out or dislodging after it is implanted.

A sketch of a typical MD-II is shown in Figure 1-1. Various regions have been defined for the dowels. The endcaps are two cylindrical disks that are at each free end. The endcaps may be distinguished from one another by the presence or absence of a driver slot and slotted driver hole. The function of the driver slot is to mesh with a surgical instrument in order to rotate the dowel into the intervertebral space. The slotted driver hole is utilized to secure the dowel to the instrument. The instrument is detached, after the dowel is implanted. The two endcaps may be described as the unslotted endcap and slotted endcap. The endcaps are connected to one another via the sidewall. An MD-II dowel contains two sidewalls. The open space within the two endcaps and the sidewall(s) is an anatomic artifact of the medullar canal. All of these regions are identified in Figure 1-1.

Allograft and autograft tissues have a well-established history in spinal fusions. However, postoperative failures are commonly reported. This is due to the variations in geometric, material, and mechanical properties of the implants. The properties of neither bone nor the products that are derived from bone are homogeneous. The intrinsic material properties of bone vary along the long axis, the circumferential and radial directions. The dimensional features of bone are not uniform. The cross-sectional area of a long bone may be tubular, oval-like, or triangular. Also, two types of bone, both cortical and cancellous, may be present in the bone stock as well as the final product. In addition there are donor to donor variations as well as variations in the processing of the tissue.

These facts create a wide range of geometric, material, and mechanical properties variations in the final MD series product line.

There are many disadvantages associated with these biological implants because of the variability. Some clinical studies discuss failures that occur after implantation of allograft or autograft interbodies for spinal fusions. Biomechanical complications associated with the interbody include extrusion (25, 152) and collapse (25, 133, 152, 159). It is reported that between 6% and 44% of failed cervical fusions are due to collapse of the interbody (25, 31, 80, 133, 152, 159). The potential complications to the patient associated with this type of malfunction may range from the mild discomfort, pain, paralysis, or even death. Collapse of the graft occurs because the applied loads exerted via the spinal column exceed the load carrying capacity of the interbody. Little research effort has been placed on insuring that these types of implants have at least a minimum level of load bearing capacity.

The purpose of this research is to propose a method based on statistical methods and fracture mechanics to define the strength of the MD-series of bone dowels and use this technique to establish a nondestructive mechanical quality control procedure. In addition, the influence of donor characteristics such as age, and sex on the strength of the dowels will be explored. The role of different tissue banking processing steps on the strength of machined tissue will be identified. Differences in strength among different dowel designs will be determined.

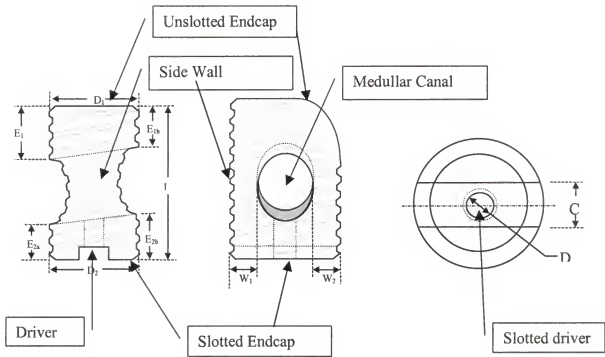


Figure 1-1. Sketch of typical MD-II bone dowel

CHAPTER 2 REVIEW OF THE LITERATURE

The Function and Anatomy of Bone

Bone performs many different functions, such as, support and protection, mineral reserve, calcium and phosphate homeostasis, blood and immunocompetent cell formation, and storage of large number of growth factors.

Soft tissue of the periosteum and endosteum cover the outer and inner surfaces of bone respectively. Bone may be grossly classified as either primary or secondary. Primary bone is present during embryonic development or fracture repair. One of the exclusive features of this type of bone is that the fibers are randomly distributed. It is also temporary and replaced by secondary bone. Secondary bone consists of cancellous and cortical bone. Cancellous bone is porous and weak compared to cortical bone. In long bones the epiphyses, the bulbous end, contains cancellous bone that is surrounded by a thin cortical layer. At the diaphysis, the midportion, it is almost exclusively cortical bone.

Bone is composed of a three dimensional polymeric organic component (Type I collagen) and inorganic hydroxapatite crystals ($\text{Ca}_{10}(\text{PO}_4)_6(\text{OH})_2$). These crystals, approximately $40 \times 25 \times 3 \text{ nm}$, lie along the collagen fibrils and are surrounded by ground substance and a hydration shell. The long bones contain rings called lamellae that compose the outer and inner surfaces. Between the inner circumferential lamellae and outer circumferential lamellae are the interstitial lamellae. Other microstructural features of long bones include the Haversian canal, which is in turn formed by cellular activity of

osteoclasts and osteoblasts. These canals traverse the bone in a longitudinal direction and are connected by numerous lacunae and even smaller canals called canaliculi.

Volkmans canals run transverse to the Haversian canals. These microscopic features result in anisotropic mechanical properties in that the properties vary in different directions.

Bone is in an equilibrium state of bone resorption by osteoclasts and bone formation by osteoblasts. It is estimated that as much as 10% of the human skeleton is remodeled annually (72). There are many local and systemic factors that control this process such as mechanical stress, electrical signals, the condition of the orthotopic site, the presence of agents that suppress bone remodeling such as non-steroidal anti-inflammatory agents, or malnutrition (59).

When bone fracture occurs, a local hemorrhage and blood clot appear forming a callus which is eventually removed during repair by macrophages. The endosteum and periosteum produce osteoprogenitor cells and cellular tissue surrounds the fracture site. This is followed by trabeculae of primary bone connecting the fractured ends and forming a callus. Physiologic applied loads eventually remodel the callus to the anatomic features prior to fracture and, secondary bone replaces the primary bone.

Transplanted bone dies but is remodeled in a similar process termed "creeping substitution". The host reorganizes the transplant by the invasion of vessels and cells, endosteum, marrow and other tissue. The surgeon (72, 116) relies on the resorption, revascularization, osteoconduction, and osteoinduction as well as the fracture repair (74) process to create a solid union in order to fulfill the goal of the surgery.

The ability of a material to enhance the bone healing process has been described by three distinct properties (41). These properties are described as osteogenic potential, osteoconductivity, and osteoinductivity. Osteogenic potential is described as the “ability of the graft to make bone” (72). In order for a graft to possess this property certain cells must be present. Most implant materials including autografts do not have osteogenic potential. Osteoconductivity is described as the ability of a graft to support the healing process similar to a scaffold (72). The implant provides a three dimensional structure for invasion by the host. All autografts and allografts as well as certain synthetic porous-like structures are osteoconductive. Cancellous bone has excellent osteoconductive properties. Osteoinductivity is the ability of a graft to induce certain cells into becoming bone (72). Only autografts and certain allografts have the ability to be osteoinductive. In addition to the osteogenic properties, bone, especially cortical bone, has advantageous mechanical properties.

Mechanics of Bone

Human bone has been broadly classified into two types: cancellous bone and cortical bone. Cortical bone covers the outside surface of long bone however the thickness varies along the longitudinal and circumferential axis. The thickness is largest at the diaphysis and gradually tapers to a thin shell at the epiphyses. The humerus and femur may be generally described as tubular while the tibia has a thick knob of cortical bone on the anterior side that runs along the longitudinal axis. Cortical bone is characterized as a densely packed ceramic in a collagenous matrix. Cancellous bone is characterized by its porosity and intricate lattice network. However, the transition from cortical bone to cancellous bone is difficult to identify by visual observation. Other means of distinguishing between these two types of bone have been reported. The

density of cortical bone has been reported to be 1.85 g/cm^3 while cancellous bone has been found to be 0.307 g/cm^3 (135). Similarly, cortical bone has four times the mass of cancellous bone. The mechanical property differences between cortical and cancellous bone are large. Table 2-1 and 2-2 summarizes some of the mechanical properties regarding these two types of bone. The volume and quality of cortical bone present will govern the failure strength of products made from bone. The challenge exists in quantifying these values.

In addition to variations in the dimensional features of the cortical bone, the elastic properties of cortical bone vary not only between different individuals but also between different bones of the same individual (73). Furthermore, the elastic properties vary around its circumference. To complicate the analysis more, the elastic properties of cortical bone have been classified as anisotropic. Some report that the properties are orthotropic while others define the properties as transversely isotropic (44, 64).

The mechanical and material properties of bone have been investigated by a wide variety of researchers. The research may be roughly divided between two separate groups. The first group may be classified as focused on material property measurements of bone. In these tests, bone is evaluated under a generally accepted test method that has been established for polymers, metals or ceramics. However, it is interesting to note that an ASTM (The American Society for Testing and Materials) test method to describe the mechanical testing of bone or products derived from bone does not exist. Yet recently, ASTM has established a committee on test methods for biologic products. The second group may be classified into the structural property measurements of allograft implants.

Table 2-1 Ultimate strength of human cortical and cancellous bone

Direction (44, 135)	Tensile Strength (MPa)	Compressive Strength (MPa)	Shear Strength (MPa)
Cortical	133	195	69
Longitudinal			
Cortical Transverse	51	133	
Cortical Radial	51	133	
Cancellous	8	0.1-100	

Table 2-2 Elastic constants for human cortical bone

ELASTIC CONSTANT	Cortical Bone (44)	Cancellous Bone (73)
E1 (GPa)	12	0.614
E2 (GPa)	13.4	0.544
E3 (GPa)	20	1.202
G12 (GPa)	4.53	
G13 (GPa)	5.61	
G23 (GPa)	6.23	
v12	0.376	
v13	0.222	
v23	0.235	
v21	0.422	
v31	0.371	
v32	0.350	

There is a large volume of literature that describes the test results of cortical or cancellous bone. In fact, Cowin (44) has authored a wonderful book that describes many of the material and mechanical properties of bone. In addition, the current literature contains volumes of material that covers material and mechanical property measurements of bone. A lot of this effort has focused on elastic property measurements. This includes methods of determining elastic modulus (14, 119), elastic modulus or strength variations in anatomic location or bone type (15, 49, 54, 86), or differences in Young's modulus

between cancellous and cortical bone (121). These techniques have been investigated for clinical use such as determining the elastic property changes after hip arthroplasty (81), and correlation between mechanical properties and computerized tomography values (123). Other areas include fracture mechanics of bone (98), fractal analysis (122), and fatigue (110). Several authors have reported the changes associated with cortical bone as a function of age such as toughness (46), presence of microcracks (42, 104), and bone loss (93). Martin (94, 95) reported on several factors such as density, collagen fiber orientation, and percent mineral content that influence the ultimate failure stress of cortical bone.

Some work has been devoted to predicting the ultimate strength of bone in anatomically specific areas. Usually these regions have specific clinical relevance in which the motivation has been in identifying those patients that have a substantial risk of fracture (36, 68, 102). There are numerous failure theories available for predicting the load bearing capacity of structures. These range from the relatively simple Maximum-Shear-Stress Theory or von Mises-Hencky theory (132) for isotropic materials to the complex anisotropic formula such as Tsai-Wu (140). In addition, Cowin (43) developed a failure theory specifically for bone. However, in order to utilize these failure theories, the principal and/or shear stresses must be determined as well as the failure stresses in these directions. In order to determine the applied stress field in the cortical bone, the elastic constants, and dimensions of cortical bone must be known. In addition, the mode of loading must be properly described mathematically.

In the field of tissue banking there are a variety of conditions including material, processing, and design that may lead to material as well as structural variation in the final

product. Material may include broad descriptors of the bone stock such as donor age, sex, height, race, geographic origin, and lifestyle. Processing includes the typical industry practices such as chemical exposure, freezing, freeze-drying ethylene oxide, and irradiation. Design refers to the shape and state of the final product. Although some research effort has been devoted to exploring these effects, many of these biomechanical issues remain to be explored especially if allograft tissue is to compete with the synthetic implant market.

Mechanical testing of bone after certain treatments that are specific to the tissue banking industry have consisted mainly of compressive, tensile, or torsion testing. Many have drawn conclusions regarding other modes of loading based on the results of this testing. Torsional strength (4) (measured as a torque load not a torsional stress) was found to decrease after autoclaving however this study has many limitations for example the authors fail to report the specimen size or mass. Specimens (113) after various preservations were tested in a similar manner in torque, compression, and bending. The preservation treatments included different freezing cycles and freeze-drying while the specimens were rat femurs (torque) or rat vertebral bodies (compression). The authors concluded that freezing treatments did not affect the mechanical properties and that freeze-drying decreased the torsional strength but not compression. The limitations of this study were that the torque was analyzed as a torque load not torsional stress and that once again neither masses nor dimensions of the specimens were reported. Compression was analyzed by determining a compression stress assuming a constant cross-sectional area of 10mm^2 . A similar study (78) was performed on rat femur (bending) and vertebra (compression) after freezing or freeze-drying and loading under compression or bending.

Once again the authors conclude a reduction of strength (expressed as load not stress) without accounting for cross-section, mass, or density variations. The sample sizes for each group are small ($n=10$) and differences may exist between rat and human bone. Some authors (61) reported the material property changes that occur as freeze-dried tissue is rehydrated as well as the changes that occur after irradiation. The specimens were human tissue and machined into dogbone-like specimens (rectangular parallelepipeds) along the long axis of either the tibia or femur and tested under tension. They report that the material properties were decreased by freeze-drying but recovered completely after 8 hours of rehydration. Irradiation to 3.5Mrads in the frozen state was reported only to increase the plastic modulus. However, irradiation in the freeze-dried state and rehydration for 24 hours was found to reduce the yield stress, and ultimate strain. These authors do not report the magnitude of any of the changes in any of the properties that they measured. In addition, they do not report the associated density of the specimen and only have tested the specimens in one mode of loading. More recently Hamer (66) proposed a method for standardizing the test methodology by testing rings under a three-point bending apparatus. However, this method assumes a constant cross-sectional area, which, especially for biological materials, is usually not the case. This technique was utilized to determine differences in strength (again expressed as load), and stiffness among specimens after various treatments (67). These treatments included gamma irradiation at different levels (0.7-6.0 Mrads), freeze-thawing, and freezing and irradiation. Freezing was identified to not have an effect, while irradiation decreased the strength to a maximum of 45% of controls at 6.0Mrads. In addition, a separate study (65) was performed to assess the difference between irradiation in the frozen state versus

irradiation at room temperature. The irradiation dosage was 3.0 Mrads. The strength measured, as maximum load at failure, was found to be significantly decreased in the room temperature group. However, the authors do not mention how much time the specimens were at room temperature prior to testing. Speirs (138) described their test procedure on human malleuses and incuses that have been machined into cylinder (diameter=1.5mm, length=4.0mm), treated differently, and tested under compression. They reported the changes in ultimate compressive stress, yield stress, and elastic modulus. They identified the ultimate compressive stress was significantly decreased due to autoclaving and 1 N NaOH. Conversely, the LpH (a penicillin solution) group did not significantly affect the failure stress when compared to the controls. However they do not account for differences in density in the specimens.

Several papers (111, 112, 128) are available which summarize the current knowledge regarding the biomechanical differences in cortical bone due to a variety of factors. Many of these authors relied on the work of Bright. There exists a need to quantify how these industrial practices influence the material properties of bone under each of the orthogonal directions. In addition, a methodology to quantify the influence of extraneous factors such as density, and donor properties must be established.

Some authors have discussed the structural properties of allograft products. Most of these products are used exclusively for spinal surgery. Although a lot of mechanical problems, especially with collapse of the bone graft, have been reported for these implants, little effort has been given in assuring at least a minimum level of residual load bearing capacity. The results of this field of research will be discussed later in the section on structural properties of allograft interbodies for spinal fusion.

Historical Development of Bone as a Transplantable Material

The early pioneers in bone transplantation successfully demonstrated that bone could be utilized for a wide range of applications in osseous repair in many different anatomic locations. The types of bone that may be transplanted depend on the origin of the transplanted graft. Autografts are taken from the same subject in whom the graft is implanted. Allografts are from a different subject but the donor is the same species. Xenografts are transplants from one species to another. Currently, autograft has been designated “the gold standard.” Its osteogenic capabilities have been shown to be superior to all other materials. However, autografts have a variety of limitations (12, 87), including additional surgical time, risk of infection, pain, and/or other complications at the site. In addition, the bone stock in the patient may be inadequate for the procedure. The retrieved graft may weaken a load bearing tissue such as grafts taken from the tibia. For these reasons, allografts have become quite popular. It is estimated that over 250,000 allograft procedures occur every year. The major disadvantages of allografts are that they carry the risk of disease transmission including infection and HIV (128). In addition, the mechanical property variations may lead to mechanical complications in the host. However, if the donor and products are properly screened and the processing carried out under appropriate conditions, this risk becomes extremely small.

Several authors reference Macewen (92) in 1878 as performing the first successful allograft transplant. In 1889, Senn (131) published his findings of utilizing demineralized xenograft tissue (tibia of an ox) in order to fill osseous defects in the tibia and femur. He stated that “antiseptic decalcified bone is the best substitute for living bone grafts in the restoration of a loss of substance in bone.” Senn stated that the material was antiseptic by storing in a “solution of sublimate in alcohol 1:500 in a

hermetically sealed bottle.” In 1912, Carrel (33) published his finding on preservation of tissue in a condition of potential life. Tissues in this condition may be preserved outside the body for an indefinite time. A variety of tissues were deposited into different mediums (isotonic sodium, chloride solution, Locke’s solution, Ringer’s solution, defibrinated blood, confined human air, and petrolatum) and stored between -1°C and $+7^{\circ}\text{C}$. In addition, skin and bones procured from an infant were preserved in petrolatum and ringer’s solution and transplanted to several different patients. Carrel also expressed the need for the availability of variety of allograft tissues that are packaged conveniently for many different operative procedures. In 1923, Hass (70) demonstrated that osteoblasts may survive for as long as nineteen hours after removal from the host. In 1937, Orell (106) reported the clinical success of allografts, xenografts, and autograft that had been boiled. The grafts were utilized for filling defects, correcting deformities, implanted in the hand, foot, and spine. He also utilized boiled bone for osteomyelitis and tumors. In addition, the illustrations in his paper show several different types of machined allografts and xenografts from hard tissues. However, he did not discuss his methods for shaping these tissues. Later other researchers have utilized autoclaving as a means of sterilizing the tissue. However, heat not only eliminates the osteogenic capability of bone but also may diminish the strength (4).

Many of the early bone transplant procedures utilized tissues from amputated limbs or procured the tissues from donors in the operating room with the patient. However, these tissues were often of inferior quality for the recipient. Later research focused on methods of preserving and sterilizing tissue in more convenient forms for the

people responsible for distributing the tissue as well as the users. In addition, many investigators proposed methods of screening the donors for potential infectious diseases.

In 1939, O'Conner (105) reported his experience with merthiolate as a preservative. The tissue was preserved in sealed jars containing an aqueous merthiolate solution (1:1000) and saline, and stored in a refrigerator. He reported that he utilized this method to preserve cartilage and transplanted the grafts in 375 procedures. In 1949, Reynolds (120) advocated a similar preservation technique for bone. He stated that the healing process of "merthiolated-preserved bone was essentially the same as that of the fresh autogenous grafts." In addition, the container with the tissue may be stored at room temperature in the operating room. He reported that this tissue had been successfully utilized in over seventy patients without any patients experiencing "sensitivity" to the implant. Although, these authors provide scientific evidence that these implants may be used successfully, merthiolate contains mercury that is a well-established toxin. In addition, others report the failure rate between 13%-40% (88).

In 1942, Inclan (76) explained his results of utilizing donor bone that had been procured aseptically and submerged in citrated blood of the donor or patient and refrigerated between 37-40°F and bacteriologically controlled during preservation without explanation. In 1947, Bush (30) proposed donor acceptance criteria as well as describing methods for properly storing the tissue. The donor's history, including the following tests should be kept: source of bone, Kline or Kahn reaction (for syphilis), history of jaundice, malaria or infections, date of storage, and weight of bone. Bush also stated that blood typing or Rh factor of grafts was unnecessary. The preservations described were regular refrigeration or deep freezing. Regular refrigeration (between +2°

and +5°C) was recommended for three weeks with the bone stored in a glass screw top container and inserted into a larger bottle. In addition, rubber sheeting and gauze capped the top of the inner vessel. The bone may be preserved by deep freezing (<25°C) indefinitely in the previously described container. In 1947, Wilson (153) published his finding on utilizing bone retrieved from amputations and other surgical procedures where it would not be harmful to the donor. The tissue was stored between 10-20°F. Wilson also performed cultures and ruled out donors based on Kline, malaria, hepatitis, and other recent acute infections. Wilson stated that he believed that creeping substitution progressed easier in bone that was dried or boiled. However, he offered no scientific evidence as proof. Wilson also professed the need for tissue banks to provide tissues to large regions that were composed of many different hospitals. In 1949, Weaver (148) described his experience using banked bone. He followed Bush's suggestions but did not perform any culturing. In addition, he stated that he had shipped the tissue to other locations. The tissue was packaged in glass vials and placed in insulated containers packed with dry ice and transplanted successfully. In 1952, Cloward (39) described his experiences using banked bone for spinal fusions. His technique was to procure the tissue under aseptic conditions, place the grafts in glass jars in a solution of blood or plasma, and stored either between 0°-20°F or 36°-42°F. He stated that the blood is "an excellent culture medium, the chances of detecting the slightest contamination are greatly enhanced."

Several researchers associated with the Navy (82) provided a detailed article of their experience with lyophilized or freeze-dried bone that is stored at room temperature. They concluded that freeze-dried bone "incorporated in the same manner as fresh

autogenous bone grafts but at a slower rate.” Freeze-drying offers many advantages, including more convenient storage and ease of handling. However, the lyophilization process has been reported to degrade the structural characteristics of the graft.

More recently the American Association of Tissue Banks (AATB) held their first scientific meeting in 1977 (28). The AATB (1) provides guidelines for Tissue Banks that covers a variety of issues. These include organization, records, donor suitability, tissue procurement, processing, labeling, and storage. This standard provides detailed information regarding the donor screening for pathogens, however, it does not provide any guidelines for ensuring the structural reliability of any of these products. These standards list several methods for the sterilization, preservation, and storage of tissue. This includes cryopreservation, freezing ($< 40^{\circ}\text{C}$), irradiation (> 1.5 Mrads), chemical (ethylene oxide, ethylene chlorohydrin, or ethylene glycol), and lyophilization (ambient or less). The guideline specifically state “the following should not be used: mercurials, quaternary compounds, formaldehyde, beta propiolactone, glutaraldehyde, and chloroform.”

Irradiation of tissue in order to reduce the bioburden has been discussed in the literature (57). However, irradiated tissue has been reported to reduce the osteogenic capability and compromise the biomechanical properties by destroying the collagen. Large doses of irradiation greater than 3.0Mrads are required in order to reduce the HIV DNA to below detectable levels. As discussed earlier, the magnitude of the biomechanical effects of irradiation may depend on whether the bone is frozen, at room temperature, freeze-dried, or irradiation dosage (57). These experiments were carried out under bending loads on variable specimen geometry and were not normalized by cross-

sectional area or density. In addition, the anisotropic directions were not accounted. Cancellous bone (11) appears to be affected in a similar manner.

Cloward first explored the use of ETO (ethylene oxide) sterilization for allografts (144). However there is a lot of controversy regarding the residuals of not only ETO but also some of the by-products such as ethylene glycol and ethylene chlorhydrin that may remain in the tissue. Several reports have described the adverse clinical consequences involved in utilizing this chemical sterilent (16, 143). Surprisingly, it remains on the list of acceptable terminal sterilization procedures in the AATB Standards for Tissue Banking (1).

Indications for Spine Surgery

Over eighty percent (51, 146) of adults experience back pain. It is one of the primary reasons (129) for health care advice, hospitalization, and disability compensation. The cost associated with this condition is estimated to be 50 billion dollars annually. Fortunately, for most patients, after two weeks (51, 52), the pain subsides. However, for the rest, additional treatment may be required. This may range from conservative therapy such as bed rest or physical therapy to aggressive surgical treatment. Approximately 0.5%-2% (51, 62) of back pain patients require surgical intervention. There are approximately 100,000-450,000 lumbar spine fusions every year in the United States (34, 146). There are myriad conditions that may be indications for spinal surgery. These include but are not limited to herniated disks, spinal stenosis, trauma, infection, spondylolisthesis, degenerative conditions. A long list of indications could be constructed but Sutterlin (26, 141) has narrowed this list to five surgical goals: correction of deformity, decompression of neural elements, debridement of pathology, stabilization of the spinal column, and pain control.

Surgery of the Spine

Spinal surgery may range from the relatively simple discectomy to the complex multilevel spinal reconstruction and fusion. These techniques range from the occiput to the sacrum, and either anterior, posterior, or lateral. In addition, they may be either open or endoscopic techniques. There are numerous references (19, 21, 58, 62, 75) the reader may consult in order to review the details of these intricate procedures. Often, some type of implant is usually used in conjunction with any of these procedures in order to stabilize the spine and achieve fusion (96).

Spinal Mechanics

Several authors have studied the loading characteristics of the spinal column. Many studies have focused on the axial load carrying capacity of different vertebral levels on human cadaveric spines. Table 2-3 presents a summary of these findings.

Table 2-3 Axial load bearing capacity of different vertebral levels

Level	Mean Load (kN)	Stdev (kN)	# Specimens	Loading rate	Reference
Lumbar	6.1	3.4	32	0.64mm/s	(23)
L5	6.7	2.2	4	Not Reported	(89)
L4	5.8	2.6	5	Not Reported	(89)
L3	5.5	2.0	7	Not Reported	(89)
L2	5.5	2.2	6	Not Reported	(89)
L1	5.0	1.9	4	Not Reported	(89)
T12	4.6	1.8	6	Not Reported	(89)
T11	4.7	2.5	4	Not Reported	(89)
L4-males	5.4	1.8	7	0.1mm/sec	(17)
L4-females	4.1	1.9	13	0.1mm/sec	(17)

In addition, other researchers have explored the in vivo loading on the human spine. Table 2-4 summarizes the results of these findings.

Table 2-4 In vivo loading on the human spine

Type of Activity	Maximum Load (kN)	Reference
Standing	0.5	(101)
Sitting	1.0	(101)
Weight Lifting	3.0	(101)
Brick Laying	4.5	(48)
Heavy Lifting	7.2	(130)

Mechanics of Spine Fusion

In order to create the fusion, the motion segment must be mechanically stable and appropriate osteogenic media must be present. Benzel (21) describes the events that lead to bony fusion as a "proverbial race between the failure of the instrumentation construct and the acquisition of bony union. During fusion the instrumentation construct and its interface with bone become progressively weaker and the bony union becomes stronger."

Mechanically, the implant system must provide rigid stabilization. However, if the implant is too rigid stress induced osteopenia of the vertebral bodies and spinal degeneration of the juxtaposed disc may result. Alternatively, if the system is too supple, pseudoarthrosis may result.

Biology of Spine Fusion

There are complex interactions (41) during the fusion process with many systemic and local factor contributing. Some systemic factors include age, state of nutrition, health, and presence of bone growth factors. Local factors that may have an influence include mechanical stability, mechanical loading, and the presence of other local growth factors, and infection. Ray (118) reported the difference in bone grafts that had been prepared under different conditions. One graft was simply frozen homogenous bone, the other was inorganic bone salt, and the last was demineralized bone. They concluded that

demineralized bone was the best. The authors indicate that Senn came to the same conclusion in 1889. It was left to Urist (145) to identify one of the major factors present in demineralized bone that provides its osteoinductive properties. Urist named it bone morphologic protein (BMP). BMP is an inductive non-collagenous protein.

The other major focus has been devoted to the biology of fusion and many clinical studies examined the difference between autograft with allograft (9, 155). In some of these studies the allograft has been combined with other substances such as autograft or demineralized bone matrix. The clinical findings in the autograft group were better.

Synthetic Implants Used for Spinal Fusion

Berthold Hadra used the first implants described in the literature in 1891 (41). He utilized a wire around adjacent spinous processes. In 1915, Albee (6, 7) published fusion techniques of using autogenous bone from the tibia. Currently, numerous implant systems are available in the market that are utilized to promote arthrodesis. These may consist of intervertebral spacers such as allografts, autografts, xenografts or some other synthetic material (metallic, ceramic, or polymeric). For example, the BAK™ (8) or Moss cage are examples of metallic (Ti 6Al-4V) intervertebral spacers. The BAK™ is manufactured and distributed by SpineTech, Inc. The design loads for these implants is 9600N under axial compression (109). Both of these devices are cylindrical and allow either autogenous or allograft bone to be packed inside the cylinder. ProOsteon™ (Interpore, Irvine, CA), a coral based hydroxyapatite material, has been implanted in a goat model in the cervical spine. However, it was not recommended for human use because of the "significant rates of collapse" (158). A carbon fiber composite is currently being implanted that has mechanical performance superior to tricortical autografts and

allografts (53). In addition to the synthetic interbody, screw and/or plate or rod systems may be used to supplement the intervertebral spacers.

Bone Grafts Utilized in Spine Surgery

Albee (5) advocated some of the first techniques that were developed for spinal fusions that utilized bone grafts. He described a tibial bone graft along the spinous processes that were secured with suture. This type of procedure successfully arrests the spondylolisthesis and fuses the spine; however, the graft will not resist physiologic loading. Other procedures propose that the graft be placed between the bodies or as an interbody graft. This type of procedure subjects the graft to large compressive loads. The function (25, 31, 156, 157) of the interbody fusion is to assist in maintaining disc height, protecting nerve roots, restoring weight bearing to anterior structures, restoring the annulus fibrosis to tension, and immobilizing the unstable degenerated intervertebral disc.

Interbody Autografts or Allografts for Spine Surgery

Capener (32) proposed a method of placing a bone graft through lumbosacral bodies but concluded "the technical difficulties... precluded their trial." In 1938 Speed (137) successfully demonstrated that this type of procedure could be performed. In 1936, Mercer (99) demonstrated one of the first interbody grafting techniques. These load-bearing implants are placed between the vertebral bodies in order to achieve intercorporal fusion. In 1944 Briggs and Milligan (27) describe a fusion using autogenous chips made from excised spinous processes. They report that they were unsuccessful in obtaining an intercorpous fusion when the chips were packed between the bodies. However, they also report that in later cases they "fashion a round peg" which is driven between the two bodies. However, they do not mention the bone origin or size of this round peg. Owens

and Williams (108) report that “pain...could be prevented by building up the joint space between the adjacent bodies of the vertebra and by fusing this space to prevent motion at this joint.” Their technique was to place a 4x3x10mm size piece of bone from the spinous process between the vertebral bodies. They report clinical success in two patients. Jaslow (77) reported a similar technique in 1946. In this time period both Smith- Robinson and Cloward popularized two independent techniques for anterior cervical spinal fusions. Cloward advocated the use of unicortical cancellous dowels obtained from either a bone bank or autogenous iliac crest. Smith and Robinson proposed a rectangular keystone graft retrieved from the patient’s own iliac crest.

Dowels

In 1953, Wiltberger (154) suggested a simplified method of vertebral body fusion using a prefit dowel. Wiltberger stated that he first used this procedure for “subastragaloid galle fusion.” First the size of the dowel (either a ½ inch or 5/8 inch) is determined from preoperative x-rays. The dowel is obtained from either “bone bank bone or autogenously through the posterior superior iliac spine.” The dowel usually has a thin cortical wall and the rest is cancellous bone. Three or four dowels that are one inch long may be obtained. A mating hole is made posteriorly in the lumbar spines to be fused and either one or two dowels are placed. Wilberger stated that the double dowel technique provides a “faster and surer fusion.” Wilberger did not report any complications associated with this technique. Sacks (127) and Harmon (69) reported a similar technique but they utilized “coin” dowels that were stacked and placed anteriorly.

In 1958, Cloward (37) popularized the use of a single dowels for anterior cervical spinal fusion by advocating the use of bone bank dowels that were ½ inch in diameter that were inserted into 14mm (38) diameter holes located on the anterior vertebral bodies.

All dowels were obtained from the ilium in an anterior-superior direction. A sketch of this dowel is shown in Figure 2-1. However, he did report that one patient was operated on through a posterior approach and another patient received an autogenous dowel and several patients received multiple level fusions. Cloward reported that 42 of the 47 patients operated on by this technique were completely relieved of pain while the other 5 improved. However, the bone graft resorbed in three patients. Cloward reported that 50% of the patients developed an anterior angulation. He attributed this to "compression force applied to the anterior half of the vertebral bodies disrupts the cancellous bone resulting in a weakening of its ability to support weight in the vertical plane."

The demand for allografts has usually outstripped the supply. Alternatives such as bovine (20) bone have been investigated to determine their suitability. Several authors (100, 142), discussed their clinical results of utilizing a Cloward dowel machined from Kiel (Calf) bone. These authors reported satisfactory clinical outcomes with no unusual complications associated with the xenograft.

In 1982, Crock (45, 63), described his technique of utilizing autogenous tricortical dowels retrieved from the iliac crest for anterior lumbar interbody fusion. These were unthreaded dowels and between 25 and 26mm in length. This dowel is shown in Figure 2-2.

In 1985, Otero Vich (107) published his findings on a threaded cylindrical dowel that was between 12-16mm in diameter. These dowels were machined from both autogenous and allograft bone. Threads are placed on a standard Cloward type dowels by inserting the core through a die. An example is shown in Figure 2-3. The site is untapped except for sizes larger than 14mm. The graft is screwed into place. The

advantages of this technique are that the graft may be removed and reinserted more precisely and with ease. It may be inserted in a more controlled manner without the risk of fracturing by impact. The loads required for extrusion of the graft are larger. A series of 37 patients treated with this technique did not have intraoperative or postoperative complications. Vich reported that the smaller size dowels appeared to subside more than the larger size and attributed this to the load bearing capacity of the smaller sizes.

Currently, Cloward Instruments, Inc. (3) supplies a complete surgical set in order to machine and insert unthreaded interbody bone graft dowels. In addition, this particular graft is a primary product line for many tissue banks and is supplied to surgeons around the country.

Complications associated with this type of graft are extrusion or expulsion, collapse and subsidence. This is due to the grafts' reliance on a large volume of cancellous bone in order to resist the applied loads. This has led to mechanical problems with the graft and resulted in complications as high as 47.5% (80). In fact, the authors of this paper advocated the use of the Smith-Robinson type interbody graft over the Cloward type dowel. Others offer that this type of procedure is not rigid enough, the surface area is much less for a dowel than a rectangular Smith-Robinson type graft, or the angle of flexion required to extrude the dowel is less than a Smith-Robinson graft. In addition, the clinical results were better for a keystone graft than a dowel graft (134).

In order to address many of the limitations of the cancellous type dowels, the MD-series of bone dowels were developed at the University of Florida Tissue Bank, Inc., in 1996. Sketches of the MD-II and MD-III bone dowels are shown in Figure 2-4.



Figure 2-1. Cloward dowel



Figure 2-2. Crock Dowel



Figure 2-3. Vich threaded cancellous dowel



Figure 2-4. MD-II and MD-III cortical bone dowels

Cubes and Rectangles

In 1936, Mercer (99) demonstrated one of the first interbody grafting techniques. These load bearing implants are placed between the vertebral bodies in order to achieve intercorporeal fusion. Mercer's technique was to utilize autogenous iliac crest grafts that were placed anteriorly between the lumbosacral joint and secured with a screw. In addition, the surgery is performed on the patient who was contained in a plaster shell. This brace remains on the patient for 4 months.

In 1952, Cloward (40) published a similar technique for posterior lumbar interbody fusion (PLIF). He utilized autogenous bone from the iliac crest but preferred allograft bone. The grafts were 1.5 x 3 cm and the full thickness of the ileum. The cortical crests of the graft are located posteriorly and up to three grafts are positioned into the disc space. These were placed with bone chips onto the cleaned surfaces of the endplate. The endplates are also notched to help stabilize the grafts. Cloward also pointed out that he did not notice if the cortical surfaces of the graft subsided into the soft cancellous bone of the vertebral bodies. However, he did note that if a graft is used that is composed only of cancellous bone without any cortical bone, it crushes under physiologic load.

Smith and Robinson (125, 136), proposed shaping a 20x20x20mm piece of autogenous bone retrieved from the iliac crest to fit the anterior cervical spine. This piece of bone is horseshoe shaped and surrounded on three sides by cortical bone. The ends and one side are composed of cancellous bone. The graft is inserted by a tamper such that the cortical exterior is in a vertical position and on the anterior part of the bodies. The superior and inferior endplates have been previously countersunk to receive the graft. Care must be taken not to remove too much "hard bone" from the endplates or the graft

may sink into the soft cancellous bone of the bodies (126). A sketch of this graft is shown in Figure 2-5.

In 1981, a variation (24) of this procedure was proposed. It was recommended to reverse the placement of the graft and locate the cortical crest on the posterior side of the vertebral body and closest to the spinal canal. These authors advocated that if the graft must be trimmed to size the cancellous end is removed rather than the cortical end. This reduces the chances that the graft will extrude or collapse. Clinical results following this procedure were better than the original results (152).

In 1960, Bailey and Badgley (18) reported their findings on their technique of fusion of the cervical spine by an anterior cervical approach with an autogenous bone graft. Their technique consisted of creating a trough in the anterior bodies that is approximately $\frac{1}{2}$ inch wide and $\frac{3}{16}$ of an inch deep and the height of the vertebra. A small ledge is left on the inferior and superior bodies to hold the graft. The disc spaces are cleaned and all cartilage removed from the endplates. The bone graft is obtained from the iliac crest and spans more than one motion segment. The graft is held in place by the suturing the prevertebral fascia and by compression under physiologic loading. A sketch of this graft is shown in Figure 2-6.

The iliac crest has become the choice graft for spinal fusions. It contains the osteoconductive and osteoinductive properties of cancellous bone as well as the advantageous structural properties of the cortical wall. Currently, this graft is supplemented by internal fixation and has shown excellent results with successful fusions obtained in up to 98% of patients (79).

Complications of this type of grafts are similar to the Cloward dowels. There have been reports that the graft may extrude, collapse, and/or resorb. The findings in literature (50, 90, 133, 159) report between 6%-34% incidence of collapse and/or resorption but no significant differences between dowels or tricortical blocks.

In order to address some of these limitations, the Tangent cortical wedge was developed at Regeneration Technologies, Inc. in 1998. This implant is composed entirely of cortical bone with ridges on both the superior and inferior surface to prevent migration after implantation. A sketch of this graft is shown in Figure 2-7.

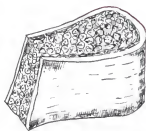


Figure 2-5. Smith-Robinson iliac crest graft



Figure 2-6. Bailey-Bagley iliac crest graft

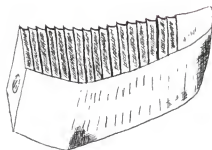


Figure 2-7. Tangent™ cortical wedge

Rings and Other Shapes

Stauffer (139) in 1972 reported that he utilized autogenous iliac crest graft for anterior lumbar fusion and these crumbled. In later cases he reinforced this iliac crest with a fibula or tibia graft. However, he did not describe the details of this assembly.

In order to confront the structural issues associated with predominantly cancellous grafts such as Cloward type dowels or Smith-Robinson keystone graphs, in 1990 Salib and Brown conceived of utilizing allograft femoral rings packed with autogenous corticocancellous chips. These grafts were maintained in place by metallic interference screws. A sketch of a typical ring is shown in Figure 2-8. Kumar et al reported on a series of 32 patients with a follow-up time between 2-4 years. Although they document that in 41% of the patients the implant was observed to subside, none of the implants were noted to fail or crack (84).

In 1997, the Cornerstone-SR graft was developed at Regeneration Technologies, Inc. This graft is ring-like and composed of cortical bone. It contains ridges on both the superior and inferior surfaces to prevent migration after implantation. It has a small cross-section in order to be utilized in the cervical spine. The graft is shown in Figure 2-9.

Other precisely machined allografts that are currently being machined by other tissue banks include the Vertigraft (Figure 2-10) machined by Lifenet and the FRA spacer that is machined by MTF (Figure 2-11). In addition, Regeneration Technologies also manufactures a large ring for the lumbar spine named the ALIF (Figure 2-12).



Figure 2-8. Cortical ring from long bone



Figure 2-9. SR™ graft

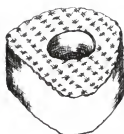


Figure 2-10. Vertigraft™

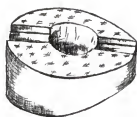


Figure 2-11. FRA-Spacer™

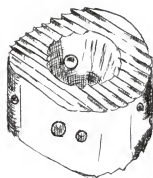


Figure 2-12. ALIF™

Structural Properties of Allograft Interbodies for Spinal Fusion

Some of the early mechanical research focused on comparing the load bearing capacity of these three different types of grafts (Cloward, Smith-Robinson, and Bailey and Bagley). They report the average loads to be 3373N (Smith-Robinson), 1912N (Bailey and Bagley), and 1507N (Cloward Dowel). Tissues retrieved from younger donors are implied to be stronger than older donors. However, the sample size was inadequate to draw any definitive conclusions regarding donor age (150, 151). Later research identified the absolute load-bearing capacity under compression as shown in Table 2-5.

Table 2-5 Load bearing capacity of various interbodies

Type of Spacer	Material	Maximum Load (kN)	Reference
Cancellous Bone	Human Allograft	0.8	(25)
Tricortical Bone - Iliac Crest	Human Allograft	2.4	(25)
Tricortical Bone - Iliac Crest	Human Allograft	5.7	(156)
Femoral Ring	Human Allograft	45.0	(117)

More recent results in the general literature have focused on predicting the biomechanical properties of this type of graft. Wolfenbarger and Zhang (156, 157, 160, 161) published a series of articles in which they attempted to identify correlation between certain physical parameters of the allograft specimens with the failure loads. These included physical, donor, or processing parameters such as freeze-drying and gamma irradiation. However, the correlation coefficients were low ($r^2 < 0.35$). In addition, they attempted to provide some guidelines to the clinician as to which graft would be most appropriate for the clinician to use. It is interesting that these authors,

who work in the tissue banking industry, recommended that the customer calculate which graft to choose rather than setting their own “in-house” threshold. Others have investigated if strength may be a function of radiographic density or anatomical location on the ileum (10, 85). However, they report that “no useful correlation was observed” (r^2 not reported) (25). Some research has focused on identifying the location within the ilium that yields the highest strength. However, none of these results is particularly useful nor have they made an impact in the tissue banking industry.

A mechanical problem is clearly evident with many of these allograft products for spinal applications. In vivo compressive loads as high as 7.2 kN may be applied to the interbody while many conventional allograft materials fail below this level. It is not surprising that many clinical studies have identified the incidence of collapse as high as 44%.

Alternative Materials to Bone

There are a wide variety of implant materials. Each material exhibits unique biologic behavior that depends on a wide range of factors. These include surface roughness, porosity, surface area, surface charge, hydrophilicity, chemical composition, extent of chemical leaching, implant size, presence of sharp corners, modulus mismatch, and wear particles (71). Typically, a fibrous capsule surrounds the implant. For metals the thickness of this capsule depends on the relative reactivity of the particular material. For example titanium and titanium alloys form thin capsules. Alternatively, some Co-Cr and stainless steels created thicker capsules. However, this is not necessarily true for polymers. Polymeric encapsulation has been attributed to the toxic chemicals that leech into the tissue from the polymers. In addition, foreign-body reactions have been reported to occur in some of the plastic systems (149). Ceramics such as Al_2O_3 are biologically

inert and exhibit extremely small fibrous capsules. Certain calcium phosphate ceramics have been considered osteoconductive. Beta tricalcium phosphate (TCP) and hydroxapatite (HA) are often used. In addition, other ceramics such as Bioglass™ (2) exhibit controlled reactions between body fluids such as fibrin, collagen fibers, or growth proteins and the materials surface to regenerate tissue. However, most ceramics are brittle and exhibit poor ductility and their use as structural implants, especially for the spine, have been limited.

Alternatives to Spinal Fusion

Disk replacement devices have been explored in a variety of different forms. Obvious mechanical advantages of that such a device would restore the spine's original mobility. Allograft motion segments have been explored in a dog model (96). Disc prosthesis have been developed such as a ball bearing, elastomeric cushions, and hydrogel cylinders. Although none of these devices have any current long-term clinical or commercial success, it is clear that a lot of resources are being devoted to the development of such a device (22).

Summary

Allografts have a rich history of being utilized for spinal fusions. However, postoperative mechanical complications have been widely reported. This is due to the applied loads exerted on the implant via the spine exceed the load bearing capacity of the graft. The tissue banking industry has focused little effort to ensure at least a minimum level of load bearing capacity of these structural implants.

The purpose of this research is to present a method based on statistical methods and fracture mechanisms to define the strength of the MD-series of bone dowels and use this technique to establish a nondestructive mechanical quality control procedure. In

addition, the influence of donor characteristics such as age, and sex on the strength of the dowels will be explored. The role of different tissue banking processing steps on the strength of machined tissue will be identified. Differences in strength among different dowel designs will be determined.

CHAPTER 3 LOCAL STRESS FIELD

Introduction

Allograft tissue, especially bone, is often implanted as structural material in many surgical procedures. These tissues may be machined into specific shapes in order to optimize their structural characteristics and add convenience to the end user. One such allograft that is commonly utilized for spinal fusions is the MD-series of bone dowels (Regeneration Technologies, Alachua, FL). These implants are primarily under two different modes of loading. Torsional loads are applied during insertion, while *in-vivo* they are primarily under axial compression. The purpose of this investigation was to examine the local stress field under simulated *in-vivo* loading and compare this to loading with a Hertzian contact load in order to identify similarities and differences between these different loading regimes.

Materials and Methods

An unthreaded 14mm MD-3 dowel without a driver slot and hole was manufactured from human cadaveric tissue. A sketch of a typical dowel is shown in Figure 1-1. An MD-III dowel contains only 1 sidewall as shown in Figure 2-4. Various regions have been defined for the dowels. The endcaps are two cylindrical disks that are at each free end. The endcaps may be distinguished from one another by the presence or absence of a driver slot and slotted driver hole. The function of the driver slot is to mesh with a surgical instrument in order to position the dowel into the intervertebral space. The slotted driver hole is utilized to secure the dowel to the instrument. The instrument

is detached after the dowel is implanted. The two endcaps may be described as the unslotted endcap and slotted endcap. The endcaps are connected to one another via the sidewall. A MD-II dowel contains two sidewalls however the MD-III dowel contains a single sidewall. The open space within the two endcaps and the sidewall is an anatomic artifact of the medullary canal.

One technique for observing the full stress field is Moiré interferometry. This well established technique (47, 115) allows direct observations of the stress gradients while under load by visually observing diffracted light. A diffraction grating is applied to the surface to be observed and the reflected light analyzed. The changes that occur in the reflection pattern are directly correlated to surface displacements. Typically, two different orthogonal in-plane directions are observed. The displacements in the horizontal or x-direction are termed the U-field while displacements in the y-direction are termed the V-field. Usually, some knowledge of the local stress field must be hypothesized, i.e. tensile or compressive, in order to identify whether or not the specimen is under an expansive or contractile displacement (47, 115).

A diffraction grating was applied to the free edge of one side of the dowel as described previously (103). A 450 Newton (100 lbf) load was applied to the specimen with an aluminum test jig as shown in Figure 3-1. The test jig consisted of two different loading platens. The radius of the first loading platen differed from the radius of the dowel by less than 0.1mm. This loading was typical of the surgical procedure and the *in-vivo* loading conditions. The radius of the second platen differed from the radius of the dowel by more than 0.5mm. The second condition is typical of the well-established Hertzian contact stress between concentric cylinders (124, 132).

The Moiré fringe pattern was observed under the compressive loading scheme as described in Figure 3-1. This fringe was observed under no load and load conditions. These patterns were observed both parallel (V-field) and perpendicular (U-Field) to the loading directions for both the *in-vivo* loading and Hertzian contact stress conditions.

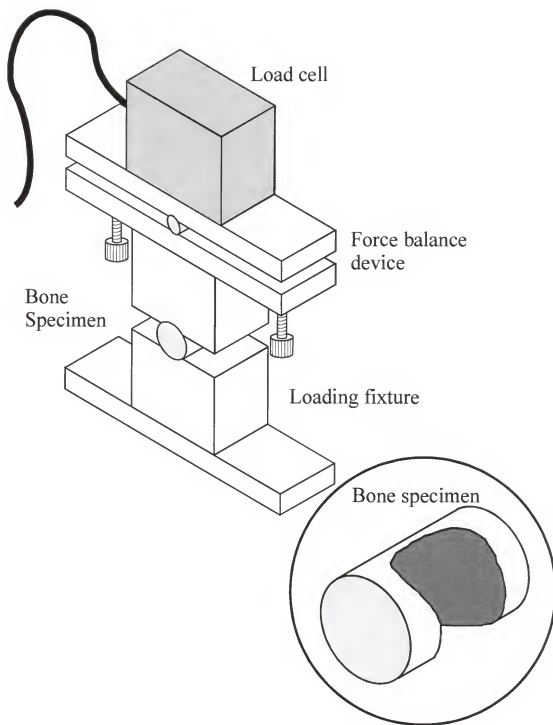


Figure 3-1 Test Jig for Moiré Loading

Results

Hertzian Contact Between Concentric Cylinders

The fringe patterns that were observed under Hertzian conditions are shown in Figures 3-2 and 3-3. The displacement fields that were observed under Hertzian contact stress show patterns typical of this type of loading (47). The V-Field (Figure 3-2) indicates a compressive loading pattern in which the contact surface is at the 12 o'clock and 6 o'clock positions. Both the 3 and 9 o'clock positions are under the smallest localized stress.

The U fields (Figure 3-3) indicates a large tensile stress below the contact surfaces (12 and 6 o'clock positions) and through the center of the specimen. Both of these loading patterns appear asymmetric and is attributed to the fact that this is an MD-III dowel and contains only one sidewall. A similar pattern observed on an MD-II with sidewalls of the same dimension would be expected to be symmetric.

In-Vivo Loading Conditions

The fringe patterns that were observed are shown in Figures 3-4 and 3-5. These patterns are different from the Hertzian patterns. The V-field, Figure 3-4, indicates that the contact surface has moved to the 2 and 10 o'clock positions on the upper loading platen and the 5 and 7 o'clock positions on the lower loading platen. The low strained regions appear to be the 12 and 6 o'clock positions as well as the 3 and 9 o'clock positions. The U-field (Figure 3-5) is similar to the Hertzian loading in that a larger tensile region is observed through the center of the specimen. However, this tensile region has shifted laterally. Once again these patterns appear to be asymmetric and are most likely due to the asymmetric specimen dimensions or asymmetric loading.



Figure 3-2. Hertzian contact stress V-field



Figure 3-3. Hertzian contact stress U-field



Figure 3-4. *In-vivo* loading V-field

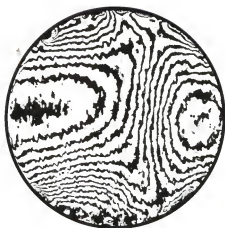


Figure 3-5. *In-vivo* loading U-field

Discussion

Other than our submitted publication, a review of the literature did not reveal any reports of applying Moiré Interferometry to bone. In addition, no other reports of applying Moiré Interferometry to Interbody implants derived from synthetic materials has been reported. However, several authors have reported finite element analysis of a cylindrical interbody under a similar loading scheme. The localized high stress fields for the *in-vivo* loading conditions were identified to be in the same location for the BAK fusion cages (109).

Ultimate failure testing of MD dowels under similar loading conditions revealed two failure modes shown in Figure 3-6. The major failure modes are visible cracks across both the top and bottom surfaces of the dowel parallel to the long axis of the dowel at this same location. In addition, another less prevalent failure mechanism was a crack parallel to the loading direction that traversed vertically through the center of the dowel on the free edge of the dowel. The first mode of failure is due to the localized stresses exhibited in the U-Field and the second mode of failure is due to the localized tensile stresses exhibited in the V-field.

There are several limitations to the current study. Simulated *in-vivo* loading was produced by utilizing aluminum blocks. This is very different from the vertebral bodies. The vertebral bodies are not homogeneous but are a functionally gradient material. The endplates are hard cortical bone while any distal movement away from the endplates the bone becomes cancellous. Therefore, depending on the placement of the interbody in either the superior-inferior or lateral-medial direction, the localized loading may be

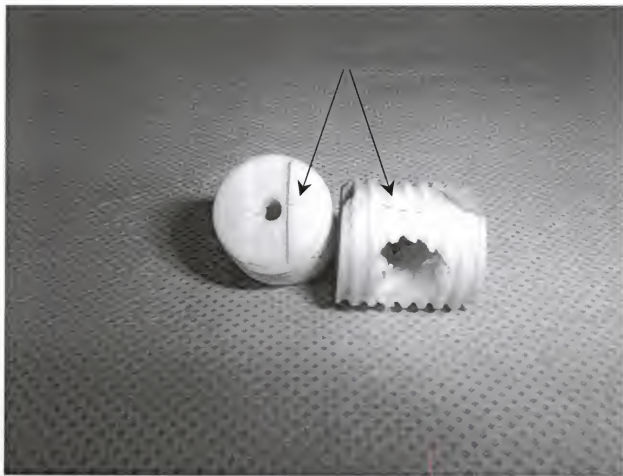


Figure 3-6 Typical fracture patterns observed in bone dowels under axial compression

different. In addition, the loads applied to the spine are complex. Multiaxial loads that involve flexion, extension, tension, compression, and/or lateral bending may be present. However, the major mode of loading is primarily axial compression.

Conclusions

This test successfully illustrated the application of Moiré interferometry on compliant cortical bone in order to identify regions of high stress. *In-vivo* loading identified similarities and differences between the *in-vivo* loading and the Hertzian loading conditions. A large tensile region was observed in both of these loading conditions. However, the compressive regions were different. The Hertzian conditions exhibited two contact surfaces while the *in-vivo* conditions exhibited four contact surfaces in which the location differed from the Hertzian conditions. These high stressed regions correlated well with the typical modes of failure observed for dowels tested to failure under axial compression.

CHAPTER 4 NORMALIZED STRENGTH

Structural Characteristics of Bone

Human bone has been broadly classified into two types: cancellous bone and cortical bone. Cortical bone covers the outside surface of long bone however the thickness varies along the longitudinal and circumferential axis. The thickness is largest at the diaphysis and gradually tapers to a thin shell at the epiphyses. A cross-sectional cut of a human femur is shown in Figure 4-1. The humerus and femur may be generally described as tubular while the tibia has a thick knob of cortical bone on the anterior side that runs along the longitudinal axis. Cortical bone is characterized as a densely packed ceramic in a collagenous matrix while notable features of cancellous bone are its porosity and intricate lattice network. However, the transition from cortical bone to cancellous bone may be difficult to identify by visual observation. Other means of distinguishing between these two types of bone have been reported. The density of cortical bone has been reported to be 1.85 g/cm^3 while cancellous bone has been found to be 0.307 g/cm^3 . Similarly, cortical bone has four times the mass of cancellous bone. The mechanical property differences between cortical and cancellous bone are large and have been identified in Chapter 1. The volume and quality of cortical bone present will govern the failure strength of products made from bone. The challenge exists in quantifying these values.

In addition to variations in the dimensional features of the cortical bone, the elastic properties of cortical bone vary not only between different individuals but also

between different bones of the same individual. Furthermore, the elastic properties vary around its circumference. To complicate the analysis even more, the elastic properties of cortical bone have been classified as anisotropic. Some report that the properties are orthotropic while others define the properties as transversely isotropic (13, 44, 64).



Figure 4-1 Cross-section of human femur

Structural Characteristics of Bone Dowels

Figure 1-1 shows uniform and symmetric dimensional attributes of the dowels. Typically, this attribute is not present in most of the dowels that are produced. A photograph of typical production dowels is shown in Figure 4-2. Notice the variation in curvature inside and outside of the medullar canal. In addition, notice the absence and presence of cancellous bone between these two dowels. These attributes lead to difficulties in accurately determining dimensional features of the cortical bone. In summary, every dowel is unique. Any technique that evaluates the strength must account for the unique dimensional variation of the cortical bone within each dowel produced.

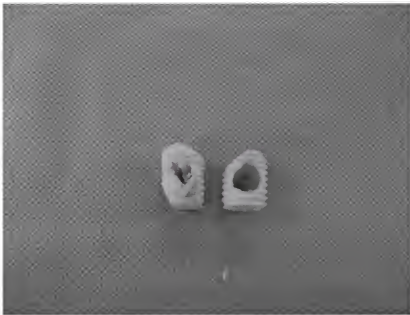


Figure 4-2 Typical production dowels

Theoretical Stress Analysis

There are numerous failure theories available for predicting the load bearing capacity of structures. These range from the relatively simple Maximum-Shear-Stress Theory or von Mises-Hencky strain energy theory for isotropic materials to the complex anisotropic formula such as Tsai-Wu (140). In addition, Cowin developed a failure theory specifically for bone (43). However, in order to utilize these failure theories, the principal and/or shear stresses must be determined as well as the failure stresses in these directions. In order to determine the applied stress field in the cortical bone, the elastic constants, and dimensions of cortical bone must be known. In addition, the mode of loading must be understood. Partly because of the difficulties involved in determining the quantities of all of these values and partly due to the initial success of empirical methods, the theoretical stress analysis has not been vigorously pursued.

Modes of Loading

The dowels are placed under a variety of service loads during its lifetime. During implantation, the dowels are primarily under torsional loading. However, *in-vivo*, the dowels are primarily under axial compressive loading. It should be recognized that if the spine undergoes flexion/extension and/or torsional loads, the dowels are under multiaxial loading. This dissertation seeks to define the strength of the dowels under axial compressive loading. All other modes of loading, if needed, will be dealt with independently in a separate document.

Specific regions of the dowel are responsible for the load bearing capacity during the different modes of loading. The sidewalls are responsible for bearing the torsional loads, while the endcaps are responsible for bearing the majority of the *in-vivo* axial compressive loads. The objective of this portion of the study was to identify the

important structural variables that correlate to the axial load bearing capacity of the bone dowels.

Materials and Methods

Specimen Preparation

The compression strength of over 1000 dowels were mechanically tested from over 900 different donors and the data compiled. All tissue was manufactured according to proprietary Regeneration Technologies Inc (RTI) processing techniques. This includes ultrasonic cleaning in chemical baths including hydrogen peroxide, and isopropyl alcohol for less than 30 minutes, packaging and frozen storage at (-20°C or -80°C). The dowels were retrieved from the diaphysis of the femur, tibia, radius, or ulna. All specimens were thawed prior to mechanical testing.

Inclusion/exclusion criteria were applied to the set of dowels in order to analyze a consistent set of specimens. These criteria included: only dowels with full and complete threads along the length of both the top and bottom surfaces; dowels with driver slot perpendicular to medullar canal and containing center hole; diameter mismatch less than 0.4mm ($|D1-D2| < 0.4\text{mm}$ see Figure 1); diameter of dowel within specifications ($D \pm 0.0-0.3\text{mm}$ where $D=16, 18, 20\text{mm}$).

Mechanical Testing

The dowels were mechanically tested to failure utilizing an MTS Bionix 858 servohydraulic mechanical test system. The maximum compressive load of this machine was 25000N. The dowels were placed in stainless steel platens that have machined grooves to match the thread profile and diameter on the dowels. The dowel was located in the middle of the fixture with the medullar canal parallel to the direction of loading. The loading ram was positioned in a machined recess in the top of the upper platen and

an initial axial compressive preload of 100N applied. Load was applied at a rate of 25mm/min and failure occurred when a change in load 1000N was detected. The orientation and loading simulated *in-vivo* conditions. Figure 4-3 illustrates the loading apparatus.

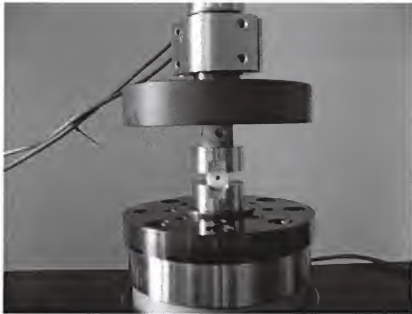


Figure 4-3. Dowel under axial compression

Physical Measurements

A variety of data was captured from the donor, donor tissue, or the dowel. Donor data included age and sex. This data was determined from the donor charts. Donor tissue data included ultrasonic velocity and anatomic location. The ultrasonic velocity may be determined by the methodologies described by Ashman (13-15). This was determined by calculating the speed of an ultrasonic signal by dividing the thickness of the specimen (to the nearest tenth of a millimeter) by the time it took the signal to traverse the specimen. Ultrasonic velocity was identified by averaging four different values 90° apart on a ring of a long bone from which the dowel was obtained. The individual responsible for manufacturing the dowel identified the anatomic location. Dowel data included size (defined by diameter), design (MD-II, MD-III, or MD-IV) endcap thickness, mass, durometry, density, length, diameter, and diameter mismatch. All dimensional measurements were determined with digital calipers. Mass was determined on a digital scale (Ohaus model LS200). Density was determined by dividing the mass by the volume (via Archimedes principal).

Donor demographics, anatomic location and the different designs will be discussed in separate chapters.

Data Analysis

The data was analyzed by a variety of different methods that are sequentially more complex. The first method analyzed the failure loads of the dowel regardless of size or design. The MD-2 and MD-3 series of dowels were separated by size from the master database. Regression analysis was utilized to identify any variable that potentially could correlate to the load bearing capacity. Lastly, a multiple regression

analysis was performed on the remaining variables to maximize the correlation coefficient (r^2).

Normalized Strength

One of the most elementary approaches to predicting failure of an object under tensile or compressive loading is to utilize the failure criterion as shown in equation (4-1).

$$\sigma = \frac{A}{CS} \quad \text{Equation 4-1}$$

Where σ is an empirically determined failure stress (usually yield or ultimate) that is unique to a material, A is the actual failure load, CS is the cross-sectional area of the material under load. The cross-sectional area depends on the geometry and is calculated from dimensional properties of the specimen. The failure is predicted to occur when

$$\frac{A}{CS} \geq \sigma \quad \text{Equation 4-2}$$

Rearranging this equation to

$$A = \sigma \cdot CS \quad \text{Equation 4-3}$$

This equation predicts the actual failure load (A) to occur when this value is equal to the predicted failure load ($\sigma \cdot CS$). In fact, this equation may be rearranged to the following:

$$\frac{A}{\sigma \cdot CS} = 1.0 \quad \text{Equation 4-4}$$

Ideally, the ratio described in equation 4-4 will be 1.0. However, deviations from ideality occur for a variety of reasons. These may include loading variations, specimen variation, processing variation, environmental variation, and mode of failure variation. Some data may fall above the line while others may fall below it. If data falls above the line, it fails above prediction and is interpreted to be strong. Conversely, if data falls below the line, it fails below prediction and is interpreted to be weak. Thus, the ratio of the actual Stress, A/CS , to the predicted theoretical stress, σ , should be 1.0. If we assume that the cross-sectional area of loading is the same, then this may also be expressed quantitatively as the ratio of actual stress to predicted stress. If this ratio is larger than 1.0, the specimen is strong. If it is less than 1.0, the specimen is weak. If it is similar to 1.0, the specimen has normal strength.

Results

Failure Load of MD-II Bone Dowels

The simplest approach was to ignore all attributes of the dowels and to examine a histogram of the failure loads of MD-II dowels. This is illustrated in Figure 4-4. Note in this Figure how the failure loads can vary between from below 10000 N to a high of 25000N. An artificial upper limit is created by the 25000 N capacity of the mechanical test equipment. Clearly, the fundamental question to answer is "why do certain dowels fail at low loads (< 10000 N) while others exceed the capacity of the mechanical testing equipment (> 25000 N). In order to answer such a question the dowels were separated by size and only MD-2s were considered.

Failure Loads of MD-II Dowels as a Function of Diameter

Dowels were separated by type and size in order to isolate the propensity for certain dowels to fail at high or low loads. The size was identified by the outer thread diameter. Examining the data from only MD-II dowels of Figure 4-4 but separating the data based on the size of the dowel reveals the histograms shown in Figure 4-6. The histogram for the 16mm dowels falls within the limitations of the testing apparatus. However, the 18mm dowels are artificially cut off at 25000N. Clearly, the size of the dowel influences the load bearing capacity. An alternate method of examining this phenomenon is to examine the average failure load as a function of the size and design of the dowel. This is shown in Figure 4-5. Statistical analysis utilizing single factor ANOVA and Fisher's multiple comparison test revealed these values to be significantly different ($p < 0.05$). The question asked in the previous section may be revised to the following: "What determines the load bearing capacity of a 16mm (or 18mm or 20mm) dowel (MD-II or MD-III)?"

Failure Load as a Function of Dimensions

One of the first empirical approaches to predict the load bearing capacity was based on the total thickness of the endcaps. The hypothesis is, if the total thickness of the endcaps is large, the load carrying bearing capacity will be large. In theory, this technique uses a simple approach with a simple measurement technique (e.g. calipers). The correlation between these two values is shown in Figure 4-7. The correlation was poorer than expected and decreased as the size of the dowel increased. The reason for this discrepancy is that difficulties arise in quantifying not only the volume but also the quality of cortical bone in the endcaps with calipers. In practice as shown in Figure 4-2, the dimensions of the endcap vary. Typically, it is a minimum along the centerline of the

cylinder and may increase (or decrease depending on the anatomy) to a maximum at the sidewall. In addition, the presence of any cancellous bone will exaggerate the readings on the calipers. Lastly, the dimensional measurements from the calipers reveal nothing about the quality of the cortical bone. Information about the cortical bone at the endcaps, such as the presence of a corticocancellous interface or porosity or the cortical bone density is not considered when measuring the dimensions of the endcaps.

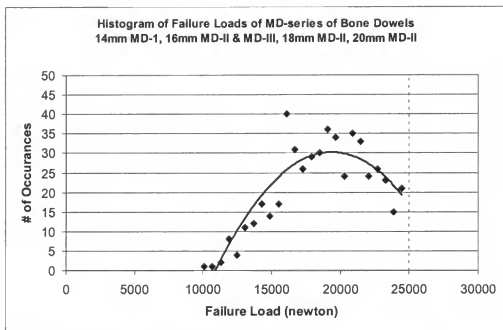


Figure 4-4. Histogram of failure loads

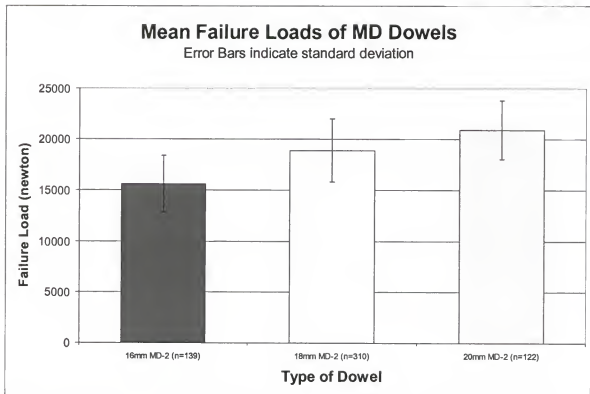


Figure 4-5. Average failure loads of different size MD-II dowels

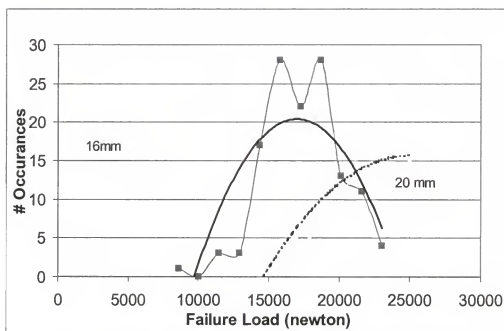


Figure 4-6. Histogram of failure loads of 16 and 20mm MD-2 dowels

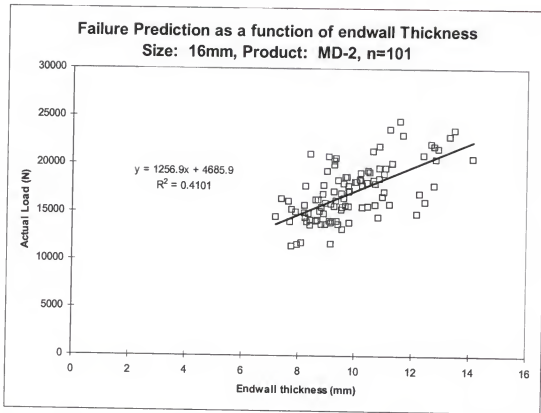


Figure 4-7. Failure load as a function of endwall thickness

Failure Loads as a Function of Density, Hardness, or Ultrasonic Velocity

Another empirical approach was to hypothesize that the load bearing capacity of the dowels is related to the quality of the cortical bone. The quality of the cortical bone was identified by a variety of different methods. These included durometry (Shore D-scale), ultrasonic velocity, and density of the dowel. A specimen that is composed of high quality cortical bone may be strong while a specimen composed of low-quality bone specimen may be weak. Density was calculated by dividing the mass by the volume, which was determined by Archimedes principle. The failure load for each of these dowels as a function of the quality measuring technique is shown in Figures 4-8 to 4-11. The correlation coefficient (r^2) for these curves are very poor. In summary, by accounting for only the quality of the bone, and ignoring details such as how much bone is available for carrying the load, will result in poor correlation of failure load with quality. A similar analogy is to examine two different metal rods. If the rods are exactly the same materials but only differ in diameter, the densities of the two are the same. However, there will be differences in compressive load carrying ability between these two rods. The magnitude of this difference depends ONLY on the difference in diameter (volume of material).

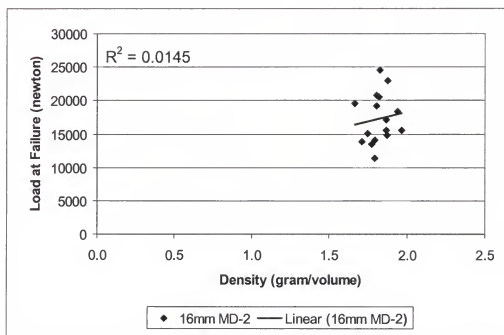


Figure 4-8. Failure load of 16mm MD-II as a function of density

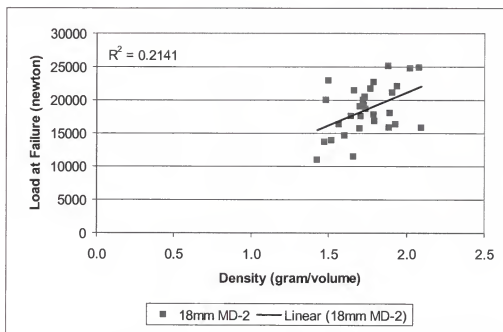


Figure 4-9. Failure load of 18mm MD-II as a function of density

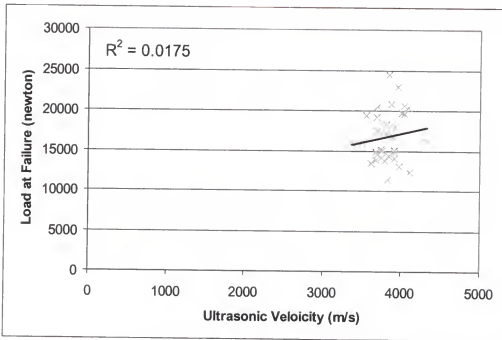


Figure 4-10. Failure load of 16mm MD-II as a function of ultrasonic velocity in cortical ring

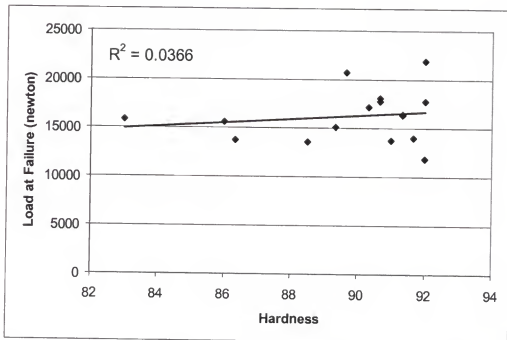


Figure 4-11. Failure load of 16mm MD-II as a function of hardness of cortical bone

Analyzing the Data by Multivariable Regression Analysis

The technique that correlates with the load bearing capacity that most successfully deals with the heterogeneous nature of the bone dowels is multivariable regression analysis. It is successful because it is able to quantitatively assess the volume and quality of cortical bone. In addition, it also accounts for loading variations due to machining differences. Several factors were considered in order to optimize the regression analysis. These included dimensional measurements (slotted and unslotted endwall thickness, diameter mismatch, and length) and mass. The other variables were not considered due to the poor correlations previously described.

A multivariable regression analysis was performed on these measurements (see appendix 1). Table 4-1 indicates the best subsets and corresponding r^2 value for three types of dowels similar results were identified for the other dowels. This table indicates that mass is the most significant predictor. The addition of the other variables contributes little to the prediction. However, in order to ensure that the specific dowel of interest adheres to RTI dimensional criteria the endcap dimensions and diameter mismatch were maintained in the equation. In summary, four variables were identified that met these criteria. These variables are as follows: Slotted endcap thickness, unslotted endcap thickness, diameter mismatch, and mass.

All of these variables may be measured directly from the dowel of interest. A regression equation takes the form of (1) below

$$\text{Predicted Load} = \beta_0 + \beta_{\text{slotted}} * x_1 + \beta_{\text{unslotted}} * x_2 + \beta_{\text{mass}} * x_3 + \beta_{\text{mismatch}} * x_4$$

where β values are the coefficients that were determined by the multiple regression analysis while the x values are determined from the dowel that is being evaluated where:

x_1 - slotted thickness in mm (00.0 mm)

x_2 - unslotted thickness in mm (00.0 mm)

x_3 - mass of dowel in grams (0.000 g)

x_4 - diameter mismatch in mm (0.0mm)

and

β values are coefficients determined from the regression analysis

x values are determined directly from the dowel of interest

The result of this regression is shown in Figures 4-12 through 4-14. The coefficients as well as the correlation coefficients are illustrated in Table 4-2. This is a large improvement in the correlation coefficients when compared to the techniques discussed previously. This technique realized r^2 values as high as 0.74. However, there appears to be a size dependence on the prediction capabilities of this technique. The prediction capability increases with decreasing size of the dowel. This phenomenon has repercussions in the Weibull analysis that will be discussed in the next chapter.

Table 4-1 Best regression subsets

16mm MD-2		16mm MD-3		18mm MD-2	
Variables	R ²	Variables	R ²	Variables	R ²
mass	0.740	mass	0.620	mass	0.455
unslotted	0.317	unslotted	0.155	slotted	0.238
mass+mismatch	0.742	mass+slotted	0.664	mass+slotted	0.470
mass+slotted	0.741	mass+length	0.630	mass+mismatch	0.456
mass+mismatch+slotted	0.743	mass+slotted+length	0.671	mass+unslotted+slotted	0.472
mass+mismatch+slotted+length	0.744	mass+slotted+mismatch+length	0.672	mass+slotted+unslotted+mismatch	0.474

Table 4-2 Regression coefficients for various size dowels

Coefficient	β_o (N)	β_{slotted} (N/mm)	$\beta_{\text{unslotted}}$ (N/mm)	β_{mismatch} (N/mm)	β_{mass} (N/gram)	(r ²)
16mm MD-2	-2588	-161	-23	1500	5078	0.74
16mm MD-3	-2769	-913	15	-2743	5874	0.67
18mm MD-2	1337	586	188	-1495	2573	0.47
20mm MD-2	4644	-415	110	1583	2587	0.42

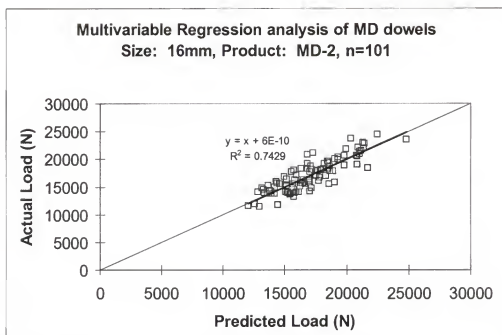


Figure 4-12. Multiple regression analysis of 16mm MD-II bone dowels

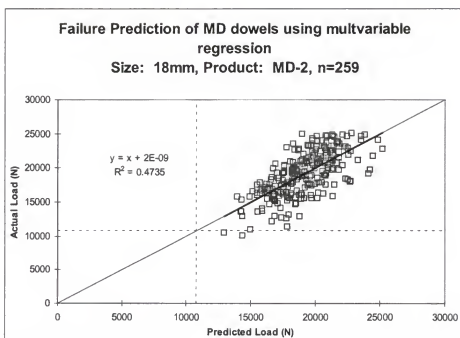


Figure 4-13. Multiple regression analysis of 18mm MD-II bone dowels

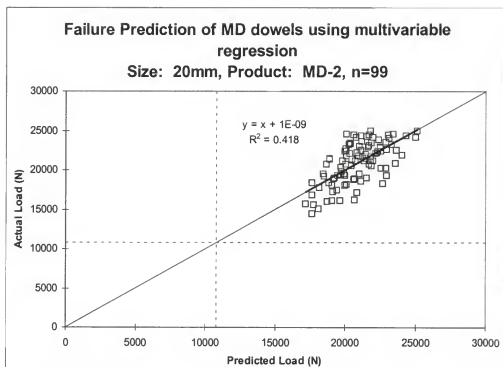


Figure 4-14. Multiple regression analysis of 20mm MD-II bone dowels

Applicability to the bone dowels

The qualitative and quantitative descriptions of strength from the section on Normalized Strength are applicable. Therefore, the strength ratio (equation 4-4) of the bone dowels is defined to be the ratio of the actual load to the predicted load.

A variety of strength behaviors are shown in nature. Generally metals have predictable strength, or simply are well behaved, and specimens derived from them would be expected to have a strength ratio of 1.0. Conversely, the strength of ceramics is controlled by the presence and the size of flaws. Because the flaw size is a Gaussian distribution, the strength is also Gaussian. The behavior of dowels is similar to ceramics; however, the cause of this behavior has not been identified. Figures 4-5 and 4-7 illustrates the Gaussian distribution for the strength of the various sizes and types of bone dowels. When designing for the strength of bone dowels, well-established techniques from the ceramics field are appropriate. In particular, the Weibull modulus technique for identifying a probability of survival or failure at a particular strength level is appropriate.

Conclusions

A systematic method of assessing the strength of the MD-series of bone dowels has been defined. This technique may be utilized for a variety of purposes. It may be utilized to assess differences in strength of the MD-series of bone dowels such as:

1. design changes to the dowels
2. immersion in solutions such as isopropyl alcohol, hydrogen peroxide
3. donor characteristics such as age, or sex
4. certain disease processes such as osteoporosis, steroid use
5. Storage variables such as freeze-drying, and/or reconstitution, freezing

6. Sterilization techniques such as irradiation, ethylene oxide, heat

In addition, this definition may be combined with a statistical treatment of fracture such as Weibull analysis to establish a biomechanical quality control procedure in order to identify any structurally deficient dowels.

CHAPTER 5 BIOMECHANICAL QUALITY CONTROL PROCEDURE

Introduction

The dowels may be placed under a range of axial compressive loads that are dictated by the age, activity level, and general health of the recipient of the dowel. In addition, the applied loads will vary depending on such factors as the spinal level where the dowel is placed, the surgical technique as well as if any auxiliary plating or rod systems are utilized. In addition, as can be confirmed in Figure 4-6, the larger diameter dowels carry more load. However, it is impractical to know which dowel will be going into which patient. Therefore all dowels must adhere to an acceptable quality criterion. This criterion is partially defined by a minimum load bearing capacity. Concomitantly, a systematic method of removing structurally deficient dowels must be explored.

The purpose of this chapter is to illustrate how the methods developed in the previous chapter combined with a quality criterion for the bone dowels may be applied to the well established Weibull technique. The Weibull analysis is often utilized to prevent failure when failure is controlled by statistical phenomena (56, 147).

Materials and Methods

Normalized Strength of Bone Dowels

Typically, strength is defined by a failure stress (either yield or ultimate). This involves normalizing the load carrying ability by dividing by the specimens cross sectional area. Unfortunately, bone dowels are not amenable to this traditional engineering approach to failure. However, the previous chapter identified a method or

normalizing the strength by multivariable regression analysis. Thus the normalized strength may be defined to be the ratio of the actual load to predicted load.

Acceptable Quality Criteria

By applying our definition for strength, identifying an acceptable quality criteria, and combining this with the statistical treatment of strength based on Weibull statistics as outlined by Wachtman or Felbeck and Atkins (56, 147), a minimum predicted load may be isolated. Any dowel that is found to have a predicted load above this value has sufficient strength to survive *in-vivo* axial compressive loads and is appropriate for implantation. Conversely, any dowel that is found to have a predicted load below this value is deemed to have insufficient strength to survive *in-vivo* axial compressive loads and is rejected for implantation.

Design Loads on the Dowels

The vertebral disk has been reported to fail at 10 000 N, while the maximum applied load on the spine has been reported to be 7200N. Based on the maximum applied load, a two-dowel construct, and a factor of safety of 3.0, a design load may be specified. This design load was determined to be 10800N ($7200 \times (3.0/2)$). This design load represents maximum static axial compressive load that potentially could be applied to the dowel *in-vivo*. It is the goal of the nondestructive evaluation (NDE) procedure to eliminate any dowel that potentially may not sustain a load of 10800 N.

Probability of Survival

Any probability may be chosen; however the lower the probability of survival the greater the risk of premature failure. The current literature advocates that when a human life is at stake, the probability of survival should be defined as 99.9999%.

Weibull Approach Applied to the Bone Dowels

A convenient approach to applying this technique to bone dowels was to separate the dowels by design (i.e. MD-II, MD-III, and MD-IV). These were then sorted by diameter. The multiple regression analysis was performed and the normalized strength (defined as the ratio of actual to predicted) was determined.

The normalized strength was sorted from smallest to largest and the natural log of the value computed. These values were numbered from 1 to n where n is the sample size. One estimate of the probability of survival can be described as noted by Wachtman (147) is

$$P_i = 1 - \frac{i - 0.5}{n} \quad \text{Equation 5-1}$$

where i is the assigned value in the numerically ranked list from 1 to n. The inverse of the probability of survival is computed and the natural log of this value is taken twice. A plot was constructed of $\text{Ln}(\text{Actual/Predicted})$ versus $\text{Ln}(\text{Ln}(1/P_s))$ and the slope (m) and intercept (b) determined. The slope represents the Weibull modulus. Once again Wachtman presents the following expression for Weibull:

$$\sigma_o = e^{-b^{1/m}} \quad \text{Equation 5-2}$$

Finally, the probability of survival may be defined by the following expression

$$P_i = \exp \left\langle - \left[\frac{(\frac{\text{actual}}{\text{predicted}}) - \text{lowlimit}}{\sigma_o} \right]^m \right\rangle \quad \text{Equation 5-3}$$

Lowlimit represents the lowest normalized strength ratio that would be expected to be observed. This value was defined to be 70% of the lowest observed normalized strength or 0.44. The details for calculating the Weibull modulus for 16mm MD-2 dowels are described in the appendix.

The goal is to isolate the threshold load in order for the dowel to survive our design criteria (i.e. 10800N load @ 99.9999%). This *threshold load* is compared to the *predicted load* (via the regression equation). If the predicted load is equal to or below this *threshold load* the dowel is rejected for implantation. If the computed predicted load is greater than the *threshold load*, the dowel is accepted for implantation. If equation 5-3 is solved for the predicted load the following expression results:

$$Predicted_{threshold} = \frac{-10800N}{\left(-lowlimit - \left(-\ln(P_r)\right)^{\frac{1}{m}} \cdot \sigma_o\right)} \quad \text{Equation 5-4}$$

Where the variables have been defined previously.

Validation

A validation was performed to ensure that the nondestructive technique effectively evaluates the axial compressive strength of the MD-Series of dowels. Comparing nondestructive analysis to destructive analysis accomplished this validation. Once validated, the nondestructive analysis can then be used as a mechanical quality control procedure to verify the strength and therefore safety of the dowels.

Specimen Preparation

Dowels were manufactured in clean rooms by typical dowel manufacturing techniques and transferred to the Biomechanics lab for testing. Two or more dowels were provided from each donor. Typically, processing personnel chose these dowels, because of their perceived sub-optimal structural characteristics. However, all dowels included in the validation study met the following criteria: There were full and complete threads across the entire length of the top and bottom surfaces of the dowel. Dowel diameter was within dowel specifications. Dowel diameter mismatch was less than or equal to 0.3mm. Diameter, and endcap dimensions as well as mass were recorded by the typical production techniques.

Sample Size

Table 5-1 illustrates the minimum sample sizes required to complete the validation study.

Table 5-1 Minimum sample size for validation

Dowel Type	Dowel Size	# of specimens	# of donors
MD-2	16	40	> 3
MD-2	18	40	> 3
MD-2	20	40	> 3
MD-3	16	40	> 3

Nondestructive and Destructive Analysis

Predicted load analysis was performed utilizing the regression equations identified in chapter 3. This value was compared to the threshold to identify a pass or fail. Destructive testing was completed using the 858 Bionix MTS Servohydraulic mechanical test machine per the methods described earlier. All data from nondestructive evaluation and destructive test were compared for final analysis.

Possible Outcomes

Comparison between nondestructive and destructive results may produce four possible outcomes as described in Table 5-2. In an ideal situation, all evaluated dowels will be correctly predicted to sustain loads above or below the design load. However, it is recognized that errors may occur. Acceptable errors mistakenly reduce the number of dowels available for transplantation. Although undesirable, acceptable errors provide a buffer between dowels with correctly predicted outcomes and those with unacceptable errors. Unacceptable errors may result in poor clinical outcomes.

Table 5-2 Possible Outcomes for validation

Nondestructive Evaluation	Destructive Evaluation	Possible Outcome
Predicted to survive 10800N	Sustain load above 10800 N	Correctly predicted
Predicted to survive 10800 N	Sustains load below 10800 N	Unacceptable error
Predicted to fail 10800 N	Sustains load above 10800 N	Acceptable error
Predicted to fail 10800 N	Sustains load below 10800 N	Correctly predicted

Acceptable Outcomes

In order for the NDE procedure to be validated, the following criteria were met. The number of unacceptable errors for each size and type were set to zero. If any unacceptable errors result, the nondestructive evaluation procedure must be revised.

Results

Weibull Modulus, Intercept and Threshold Load

Table 5-3 identifies the m , b , lowlimit, design load, and σ_0 for each of the dowels that have been analyzed. The sample size (n) used to compute these parameters is also given.

Table 5-3 Weibull analysis results for various dowels

Design	Diameter	n	m	b	σ_o	Lowlimit	Design load (kN)	Threshold load (kN)
MD-II	16	101	14	-0.5	1.0	0.44	10.8	13.0
MD-II	18	259	10	-0.5	1.1	0.44	10.8	15.3
MD-II	20	99	12	-0.5	1.0	0.44	10.8	13.8
MD-II	22	36	11	-0.5	1.0	0.44	10.8	15.8
MD-II	24	31	7	-0.5	1.1	0.44	10.8	15.9
MD-III	16	47	9	-0.5	1.1	0.44	10.8	14.5
MD-IV	18	44	9	-0.5	1.1	0.44	10.8	18.3

Plots of P_s versus Actual/Predicted may be constructed. These curves are typical of survival curves that are well documented in the ceramics literature. Plots of the 16 and 18mm MD-2 dowels are shown in Figure 5-1.

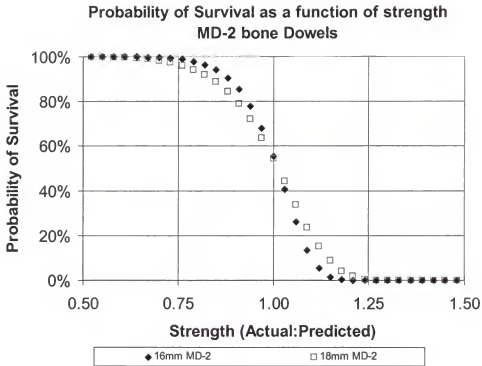


Figure 5-1. Probability plots of 16 and 18mm MD-2 dowels

It is an interesting observation of Table 5-3 and Figures 4-9 and 4-10 if the 16 and 18 mm MD-2 dowels are compared, the 18mm dowels have a average failure strength greater than the 16mm dowels. Surprisingly, the threshold load is greater for the 18mm than the 16mm MD-2. The reason for this is that the regression analysis for the 18mm has a lower correlation coefficient, which translates into a lower Weibull modulus (10 versus 14). One could deduce from Table 5-3 that the 24mm MD-2 has the poorest correlation coefficient; however the Weibull analysis allows these inequities to be satisfied by increasing the threshold.

Validation Results

Table 5-4 illustrates the results of the validation procedure. The actual number of specimens that were tested exceeded the minimum sample size. All dowels met the requirements described in the study design. Out of the 606 dowels tested, 590 dowels (97.4%) were correctly predicted to sustain loads above the design load and 16 dowels (2.6%) were predicted to fail at the design load but actually sustained loads above the design load (an acceptable error). As required, zero unacceptable errors resulted.

Table 5-4 Validation actual outcomes

Type	Dowel Size	# of Dowels	# of Donors	Correctly Predicted to Pass	Correctly Predicted to Fail	Acceptable Error	Unacceptable Error
MD-2	16	104	89	101	0	3	0
MD-2	18	215	201	203	0	12	0
MD-2	20	188	171	188	0	0	0
MD-3	16	99	86	98	0	1	0

Results in Manufacturing Since Implementation of NDE at RTI

In July of 1998, RTI evaluated 7,027 dowels by this procedure. Of these, 6,869 (97.8%) of the dowels met or exceeded both dimensional and structural loading

requirements. 133 (1.9%) dowels failed for dimensional reasons while 25 (0.3%) failed for structural reasons. The average predicted load for the MD-Series dowels is 1.44 times stronger than the minimum threshold.

In addition, 13 dowels that were rejected by the NDE procedure were retrieved and destructively tested. 2 of these 13 failed below 10,800N. These rejected dowels had an average failure load of 12,725 N. MD-II and MD-III dowels sent to the Biomechanics lab for destructive evaluation fail at an average of 17,067 N (16mm MD-II) and 18,297 (16mm MD-III).

It should be noted that these 13 dowels met all dimensional requirements and could have been released as product if the nondestructive evaluation procedure was not in place.

In October of 1999, a histogram of the predicted loads of the 16mm MD-2 dowels (n=8134) that have been evaluated since the process was adopted by RTI was plotted and is shown in Figure 5-2. Plots of 18 and 20mm MD-2 dowels are similar. The threshold predicted load for this size and design (13029N) is also shown on the plot. It is clear that many of the dowels that are manufactured by RTI are well above the acceptable quality standard that has been established for the dowels.

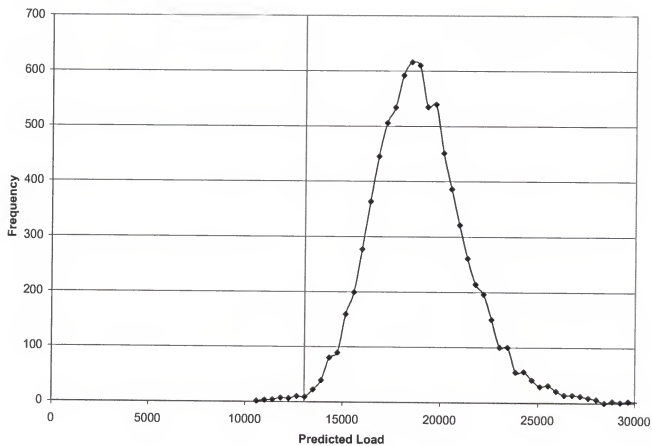


Figure 5-2. Typical results when applied to manufacturing environment for 16mm MD-2

Conclusions

An acceptable quality criterion can be identified for allograft materials.

An empirical treatment of failure identified by regression analysis may be successfully combined with a quality criteria and Weibull analysis in order to establish a nondestructive quality control procedure.

The nondestructive evaluation procedure was successfully validated. This process accurately predicts whether or not a MD-Series of dowels will survive axial compressive design loads.

CHAPTER 6 PROCESSING AND DONOR DEMOGRAPHICS OF CORTICAL BONE

Introduction

Allografts have a well-established history as implantable materials for structural applications. Frozen storage hinders the material for many potential applications. This method requires the tissue to be maintained in expensive -80°C freezers prior to implantation. Many surgical sites do not have access to such freezers, which requires the implants to be shipped on dry ice, immediately before their use. More convenient preservation/sterilization processes are available but the relationship between the process and the ultimate strength of the tissue is not well understood. Two processes that tissues are frequently subjected to are sterilization by gamma irradiation and/or preservation via lyophilization. Lyophilized tissue may be stored at room temperature. In addition, the tissue may be derived from donors from an elderly population.

The results in the general literature are inconsistent. Some researchers state that there is not an effect on strength from irradiation (60, 160). Others report that the effect of irradiation depends on dose, mode of loading, and/or state of the tissue (91, 111).

Bone is an anisotropic composite material. Because of this fact it is important to identify the strength of bone in different directions. In addition, allograft products may see a variety of loading modes during their service. Typically, shear loads are present during insertion or implantation of certain allograft products such as the torque applied to a bone dowel interference screw. Axial compression (parallel to the long axis) is often

the preferred *in-vivo* loading mode because this is the bone's strongest direction.

Likewise, transverse tension is important because it is the weakest direction.

The objective of the study discussion in this chapter was to investigate how allograft processes such as freeze-drying, irradiation, autoclaving, and/or rehydration alter the ultimate strength of the tissue. In addition, certain specimens were treated with BioCleanse™, a proprietary viral inactivation process developed by Regeneration Technologies, Inc. Cylinders of cortical bone were subjected to three different modes of loading and described as follows: axial compression (loaded parallel to long axis), shear (loaded perpendicular the long axis in double lap shear), and transverse tension, (loaded perpendicular to the long axis under diametral compression). In addition a separate group of specimens that were derived from females between the ages of 70-80 were also tested.

Materials and Methods

Specimen Preparation

Compression and transverse tension specimens were isolated from 18 human donors (5 females and 13 males) with an average age of 54 years (Range: 18-67 years). The tissue was machined into cylinders with a mean diameter and length of 4.0mm and 5.5mm respectively (compression) and 4.0mm and 5.9mm respectively (transverse tension). Each donor yielded approximately 25 and 35 cylinders for compression and transverse tension respectively. Shear specimens were isolated from 9 human donors (2 female, 6 male, 1 unknown) with an average age of 49 years (Range: 19-75 years). The tissue was machined with a lathe into 181 pins that were 2.0mm in diameter and 20mm in length. Each donor yielded between 17 and 22 pins.

Ten representative older female donors with an average age of 75.7 (Range: 70-80) were chosen to compare the strength of this population to the strength of the other groups.

Additional testing was performed under shear to compare the difference between pins that were 1.5mm in diameter to 2.0mm in diameter. These pins were derived from 6 donors (1 females, 4 males, 1 unknown) with an average age of 46 years (Range: 23-66 years)

All specimens were retrieved from the cortex of the femur or tibia and all cancellous bone was visually confirmed to be removed from the surface. The premachined tissue was soaked for 20 ± 5 minutes in 3% hydrogen peroxide. All specimens were maintained frozen at least -20°C except during specimen preparation, testing, or after freeze-drying. During the machining process tissue hydration was maintained with a 0.9% NaCl solution.

Experimental Design

The study was parallel arm and designed to detect a 15% difference in strength among the different treatment groups (compression and transverse tension) or between control and treatment groups #2-#7 (shear). Significance level (α) and power ($1-\beta$) were set to 0.05 and 0.90 respectively. Under these assumptions, the specimen size for each group was to be 50 (compression) or 75 (transverse tension) or 68 control and 18 per treatment (shear). Estimates were made of the sample sizes for the older female donors (group #10) as well as shear pins in groups #8 and #9.

Significant differences were detected in the axial and diametral compression specimens by ANCOVA utilizing the density of the bone as a covariate. Neuman-Keuls

tests with Kramer's modification was utilized as a multiple comparison test to detect differences among the various different treatment groups. Shear specimens were analyzed by ANCOVA however Dunett's Test with Kramer's modification was used to detect significant differences between physiologic and treatment group.

Treatment Groups

The pins were randomly assigned to the treatment groups as described in Table 1 (compression), Table 2 (shear), and Table 3 (transverse tension). Each pin was stored in a sealable container after machining. Control specimens were stored frozen but thawed to room temperature prior to testing. Freeze-drying (FD) was performed by standard methods in a lyophilizer (Vertis Gardiner, NY) and sealed at 100-200 mTorr in a glass vial that maintained the low pressure. The irradiated (Irr) specimens received between 1.5-2.5 Mrad or 3.0-3.5Mrad (Food Technology Services, Inc, Mulberry FL). The irradiated only specimens were maintained in dry ice during the entire shipping and irradiation process. Autoclaving was performed for 30 minutes at 250°F with the specimens sealed under the low pressure in a glass vial. BioCleanse™ was performed at RTI. Lastly, reconstitution (recon) was performed with 0.9% NaCl in a partial vacuum for at least 24 hours prior to testing.

Table 6-1 Axial compression treatment groups

Group	Treatment
1	Physiologic
2	FD
3	FD + Recon
4	FD+Irr (1.5-2.5 Mrad)+Recon
5	FD+Irr (3.1-3.5 Mrad)+Recon
6	FD+irr (1.5-2.5Mrad)+autoclaved+Recon
7	frozen & irr (1.5-2.5Mrad)
8	frozen+irr(3.1-3.5Mrad)
9	Biocleanse
10	Older females 70-80 years

Table 6-2 Shear treatment groups

Group	Treatment
1	Physiologic
2	FD
3	FD+Irr (1.5-2.5 Mrad)
4	Frozen+Irr (1.5-2.5 Mrad)
5	FD+Recon
6	FD+shipped+recon
7	FD+irr (1.5-2.5 Mrad)+shipping+recon
8	1.5mm Physiologic
9	2.0mm Physiologic
10	Older females 70-80 years

Table 6-3 Diametral compression treatment groups

Group	Treatment
1	Physiologic
2	FD
3	FD+recon
4	FD+Irr (1.5-2.5 Mrad) + recon
5	Frozen +Irr(1.5-2.5 Mrad)
6	Frozen+Irr(3.1-3.5 Mrads)
7	Biocleanse
8	Older females 70-80 years

Physical and Mechanical Testing

Prior to lyophilization the mass, diameter, and length of each specimen were determined. The density of each specimen was calculated by dividing the mass by the volume (determined by assuming the volume of a perfect homogenous cylinder). Mechanical test methodologies were adapted from ASTM D695-91 (compression), ASTM B565-94 (shear), or ASTM C496-90 (diametral compression) and performed on an MTS 858 (MTS Systems Corp, Eden Prairie, MN) servohydraulic mechanical test apparatus. Ultimate strengths were determined by the following expressions:

$$\sigma_{compression} = \frac{P_{max}}{\pi \cdot (d/2)^2} \quad \text{Equation 6-1}$$

$$\sigma_{transversetension} = \frac{2 \cdot P_{max}}{\pi \cdot d \cdot l} \quad \text{Equation 6-2}$$

$$\sigma_{shear} = \frac{2 \cdot P_{max}}{\pi \cdot (d/2)^2} \quad \text{Equation 6-3}$$

where P_{max} is the maximum load, and d and l are the diameter and length of the specimen respectively. Load was applied under displacement control and applied at 25mm/min. Figure 6-1 and 6-2 illustrate the testing apparatus.

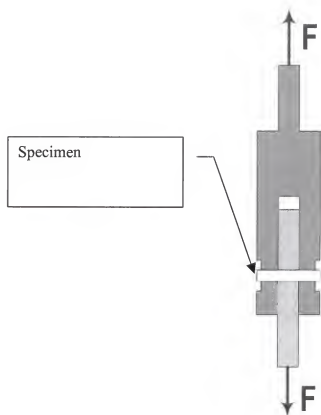


Figure 6-1. Shear Test Fixture

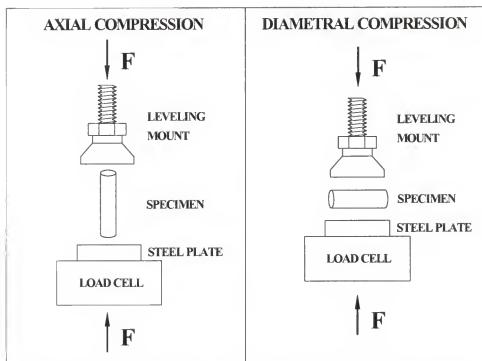


Figure 6-2. Test configuration for axial and diametral compression

Results

Tables 6-4 to 6-9 describes the sample size (n), mean, standard deviation (SD), minimum and maximum density and ultimate stress measurement for each of the treatment groups under the different modes of loading.

Table 6-4 Density of each compression group prior to treatment

Group	Density (g/cm ³)			
	Mean	SD	Minimum	Maximum
1 (n=51)	1.88	0.08	1.62	2.04
2 (n=52)	1.87	0.08	1.66	2.05
3 (n=53)	1.88	0.07	1.71	2.01
4 (n=51)	1.89	0.09	1.59	2.04
5 (n=53)	1.89	0.07	1.64	1.98
6 (n=50)	1.89	0.08	1.66	2.01
7 (n=49)	1.88	0.09	1.66	2.01
8 (n=51)	1.89	0.09	1.62	2.13
9 (n=51)	1.89	0.07	1.67	2.05
10 (n=131)	1.89	0.10	1.13	2.30

Table 6-5 Ultimate compressive strength of each treatment group

Group	Axial Compression (MPa)			
	Mean	SD	Minimum	Maximum
1 (n=50)	204	24.5	151	272
2 (n=51)	303	75.9	159	469
3 (n=50)	169	19.6	126	207
4 (n=51)	161	16.3	111	181
5 (n=53)	157	15.3	96	180
6 (n=50)	167	18.3	107	188
7 (n=49)	229	27.9	145	298
8 (n=51)	223	27.8	134	268
9 (n=51)	203	36.1	111	315
10 (n=131)	165	17	116	202

Table 6-6 Density of each shear group prior to treatment

Group	Density (g/cm ³)			
	Mean	SD	Minimum	Maximum
1 (n=68)	1.83	0.14	1.37	2.01
2 (n=19)	1.81	0.14	1.55	1.96
3 (n=19)	1.88	0.14	1.57	2.02
4 (n=19)	1.80	0.18	1.45	2.05
5 (n=19)	1.87	0.16	1.43	2.12
6 (n=19)	1.86	0.12	1.58	2.06
7 (n=18)	1.84	0.12	1.58	1.96
8 (n=27)	2.00	0.13	1.82	2.27
9 (n=29)	1.91	0.09	1.72	2.13
10 (n=150)	1.88	0.11	1.57	2.02

Table 6-7 Ultimate shear strength of each treatment group

Group	Shear (MPa)			
	Mean	SD	Min	Max
1 (n=68)	84.7	16.2	46.2	116.3
2 (n=18)	60.3	15.0	30.5	86.1
3 (n=19)	51.5	16.9	23.9	79.3
4 (n=18)	63.1	11.0	35.7	77.2
5 (n=19)	67.0	13.8	33.8	98.8
6 (n=19)	66.2	13.5	36.3	92.6
7 (n=18)	70.9	10.6	47.1	81.6
8 (n=22)	98.5	11.6	81.3	125.9
9 (n=29)	70.0	8.1	47.1	84.5
10 (n=150)	59.5	7.3	40.0	76.5

Table 6-8 Density of each transverse tension group prior to treatment

Group	Density (g/cm ³)			
	Mean	SD	Minimum	Maximum
1 (n=80)	1.88	0.07	1.74	2.09
2 (n=81)	1.90	0.07	1.66	2.08
3 (n=80)	1.89	0.06	1.61	2.00
4 (n=83)	1.91	0.06	1.68	2.03
5 (n=79)	1.89	0.05	1.72	2.05
6 (n=80)	1.87	0.06	1.69	1.99
7 (n=76)	1.91	0.05	1.75	2.10
8 (n=137)	1.90	0.06	1.63	2.03

Table 6-9 Ultimate transverse tensile strength of each treatment group

Group	Transverse tensile strength (MPa)			
	Mean	SD	Min	Max
1 (n=79)	29.0	5.0	19.0	45.2
2 (n=81)	31.8	10.1	11.4	54.0
3 (n=80)	24.7	5.3	15.2	52.6
4 (n=83)	21.5	4.2	7.5	33.1
5 (n=79)	27.1	4.8	16.7	38.4
6 (n=80)	25.5	4.5	17.1	44.0
7 (n=76)	29.2	4.6	19.8	41.9
8 (n=130)	26.1	5.0	12.0	52.3

Previous research identified a correlation between the strength of cortical bone and its density (94, 95). The density of the control group was found to be 1.88 g/cm^3 (compression), $1.83 \pm 0.14 \text{ g/cm}^3$ (shear), and 1.88 g/cm^3 (transverse tension). Prior to processing statistical analysis revealed that differences did not exist in the average density of any treatment group under any of the axial or diametral compression groups. In addition, there were not any statistical differences between shear groups 1-7 and 9. However, group #8 was found to be statistically different from all others.

For the compression testing significant decreases ($p < 0.05$) were observed in groups #3, #4, #5, #6, and #10. Group #2, #7, and #8 significantly increased ($p < 0.05$) the compression strength. No differences were detected in group #9 specimens. In addition, the variability of the freeze-dried specimens (#2) increased by a factor of 3 when compared to the controls.

For shear testing, treatments #2-#7 were found to significantly decrease the shear strength ($p < 0.05$) when compared to the control group. #9 was found to be less than #1 and cannot be explained. #8 is larger than #9 and is attributed to a size effect on the pins.

No statistical assessment has been made among treatments 8, 9, 10 and all other treatment groups.

The 1.5mm pins have higher density and therefore higher shear strength. The older female donor group was found to be weaker than the controls.

For transverse tensile testing, treatments #3, #4, #5, #6, and #8 were found to significantly decrease the transverse tensile strength ($p < 0.05$) when compared to the control group. No differences were detected in group #7 specimens. #2 was found to be greater than the controls ($p < 0.05$).

Discussion

Cowin (44) tabulated the results from a variety of different sources under a variety of loading conditions for human bone. These tables indicate that the ultimate strength of the human femur or tibia to be between 131–224 MPa (compression), 53–76 MPa (shear) and 9.9–51 MPa (transverse tension). All of our values for bone in the physiologic state fall within the ranges documented by Cowin except for groups #1 and #8 under shear specimens. Group #8 is most likely due to the higher density cortical bone. However, differences may also be due to testing methodologies. Cowin reported that the shear strength was determined by testing the specimens under torsion while ours were tested under double lap shear.

Bright and Burchardt (61) were some of the first investigators to report on biomechanical changes associated with freeze-drying and irradiation of tibia and femoral bone. They tested rectangular parallelepipeds under both tension and compression. They state that the modulus is restored after 1 hour, yield and ultimate stresses restored after 4 hours and ultimate strain after 8 hours. However, they do not report if the reconstitution was performed under low pressure or atmospheric pressure. He also reports that the only

property that was altered when the specimens were irradiated at 3.5Mrads was the plastic modulus. However, he did not state whether the specimens were irradiated at room temperature or frozen conditions. In addition, they state the specimens that were irradiated under the freeze-dried state and subsequently rehydrated did not recover their yield, or ultimate strain. They did not mention how the ultimate stress is altered.

Pelker (113) reported on the effects of freeze-drying and subsequent rehydration in saline for 24 hours. The specimens were rat femurs and tested under torque. They report that the freeze-dried rehydrated specimens were significantly weaker (50% of controls, measured as torque not shear) than the controls. They also report that the freeze-dried specimens were placed in an oven at 100°C until a constant weight was achieved. They did not report how long these specimens were maintained in the oven.

Some research has focused on the effects of freeze/thawing on the mechanical properties. Pereira (114) noted that when whole femurs were frozen (-70°C or -150°C) and thawed at a controlled rate (1 °C/sec) that cracks were visible on radiographic examination. These cracks ran parallel to the long direction of the bone and were adjacent to the nutrient foramen. However, they tested whole femurs and noted that if the intermedular contents are removed, stress fractures may be avoided.

Irradiation has been reported by Hamer (65) to affect cortical bone by destroying the collagen. They describe their results of mechanically testing ring specimens under three point bending. Their treatment groups were irradiation (3.0Mrads) under either room temperature or on dry ice. They did not test a control group. They report that the room temperature irradiated group failed at 84% of the failure load (not stress) of the frozen group. They also report that the degree of collagen denaturation was significantly

less in bone irradiated while frozen. It is difficult to compare our mechanical test results to this study because our mode of loading is different. Hamer (67) reports in a separate study that specimens irradiated (3.0Mrads) at room temperature reduced the failure loads to 64% of controls (determined by load not stress). Although, these authors have large sample sizes from 6 cadaveric femurs, they use unusual specimen geometry (ring) and do not account for geometric (dimensional) or physical differences (density) of the specimens.

Kubler (83) did a series of compression testing on human bone. Their specimens consisted of cylinders (4mm diameter and 6mm long) machined either parallel or perpendicular to the long axis of the bone. They treated the bone with typical tissue bank processes, lyophilization with and without rehydration as well as with and without surface demineralization in 0.6N HCL until they estimated (by scraping with a scalpel) the demineralization depth was 1mm. For the bone loaded parallel to the long axis, they report that the compressive strength of the controls was 106MPa. The freeze-drying increased the compressive strength of bone by 130% (244MPa). The rehydrated lyophilized bone recovered back to its physiologic state. The surface demineralized lyophilized with and without rehydration was documented to have approximately the same compression strength (118MPa vs 112MPa). They report similar results for the specimens machined perpendicular to the long axis. Some of our results differed from their results. They did not report their rehydration regime. In addition they only had 10 specimens per treatment group. They did not provide details where these specimens were derived (i.e. humerus, radius, ulna, tibia, femur, sex, and age) or did they confirm the pretreatment densities.

Freeze-dried tissue is often packaged in glass vials with rubber stoppers and shipped to the users in sets of multiple grafts individual packaged in separate vials. Often the users will inadvertently place the unused and unopened tissue through an autoclave cycle. The purpose of our investigation was to assess the effects of this autoclave cycle on the biomechanics of the graft when they are stored in the glass vial. Several different authors have reported on the effects of autoclaving on the mechanical properties of allografts. Speirs (138) reported strength differences in human auditory ossicles that were 4.0mm in diameter and 7.5mm long. These specimens were divided into four groups: control, exposure to 1 N NaOH, for 60 minutes at room temperature, exposure to 0.9% LpH for 60 minutes at room temperature and autoclaving at 134°C for 60 minutes. They examined differences in yield stress, ultimate stress, and elastic modulus. All treatment groups except for the LpH groups were significantly decreased from the controls. They report that the autoclaving reduced the ultimate compressive strength by 80%. Kreicbergs and Kohler (4) report the loss in strength is dependent on the autoclave cycle. They tested their specimens under torque after the specimens were exposed to the following autoclaving cycles: 110°C for 255 minutes, 121°C for 20 minutes, and 131°C for 2 minutes. They state that when compared to controls the strength decreased to 0.65 (110°C), 0.77 (121°C), and 0.91 (131°C). Our results for the autoclaved specimens did not reveal such differences in strength. This is most likely due to the decreased autoclaving time as well as the bone being prelyophilized prior to autoclaving. In addition to the fact that the specimens were stored in glass beaker at low pressure that insulated the specimen from the heat of autoclaving.

The strength of cortical bone is altered by the age of the donor. The tensile modulus and ultimate tensile strength has been reported to decrease 2% per decade after the second decade of life. This results in less energy to failure or a more brittle material (135). The hypothesized cause of this effect has been attributed to increased cross-linking by non-enzymatic glycation in bone collagen (35). Crosslinking of bone collagen has been reported to increase rapidly from birth to 25 years, thereafter there is a steady and but persistent increase in crosslinking density (measured in individuals up to 80 years) and reported to be independent of sex (55).

Burstein (29) tested tibia and femoral specimens of male and female tissue from both the tibia and the femur from donors between the ages of 21-86 years old. Specimens were tested in tension, torsion, and compression. All specimens were covered and stored to at least -20°C except during handling. Specimens were machined into either square cross-sectional bars or dumbbells with the long axis parallel to the long axis of the bone. In addition, certain extraneous factors such as normal donor tissue, osteoporotic, and corticosteroid-treated individuals were considered in the analysis of the data. They report approximately a 2% drop per decade in both ultimate tension and compression for the femur from the second decade ($\sigma_{\text{tension}} = 140 \text{ MPa}$, $\sigma_{\text{compression}} = 209 \text{ MPa}$) to the eighth decade ($\sigma_{\text{tension}} = 120 \text{ MPa}$, $\sigma_{\text{compression}} = 180 \text{ MPa}$). The data for the tibia exhibited a less pronounced change under tension -1.2% drop per decade but loss of compression strength was similar. The reported strength of the tibia in the second decade was $\sigma_{\text{tension}} = 161 \text{ MPa}$, $\sigma_{\text{compression}} = \text{none reported}$ while the eighth decade was $\sigma_{\text{tension}} = 156 \text{ MPa}$, $\sigma_{\text{compression}} = 197 \text{ MPa}$. Ultimate shear strength for the torsion specimens was not reported. data. The strain to failure also was reported to decrease approximately 5% to 7%. This

indicates that the aging process makes cortical bone more brittle. Burstein hypothesizes that this is due to changes that occur in collagen. Lastly, they report no consistently different properties when compared with the means of bones of the normal individuals in the same decade for both the osteoporotic as well as steroid treated individuals. Lastly they report that the ultimate stress of the tibia is significantly higher than the femur.

Several limitations are evident in Burstein's study. Although, the samples sizes are large (as high as 44 per decade), the number of donor tissue per decade is small (as small as 0). Physical differences in the specimens such as density were not reported.

McCalden (97) studied the mechanical effects of cortical bone and attempted to correlate differences in strength with donor age as well as material analysis. Specimens and testing was similar to Burstein's methodology (29). However, only right femurs were retrieved from donors between the ages of 20-102 from twenty-five males and twenty-two women. Ultimate tensile strength was identified to decrease at 5% per decade from the second decade ($\approx 140\text{MPa}$) to the tenth decade ($\approx 75\text{MPa}$). Elastic modulus showed no change however ultimate strain as well as plastic energy were reported to decrease as a function of age.

The ultimate tensile stress was shown to be unrelated to sex, mineral content (ash weight), and calcium content. However, the mineral content in their specimen population was narrow and if cortical specimens from other species or locations that have a mineral content outside of their range were compared, differences may exist. Alternatively, the data indicates that the failure stress is highly correlated to the porosity of the cortical bone. The authors state "...the major determinant of strength in aging bone is the amount of bone in cross-section that is available to resist the tensile stress." Porosity decreases

the effective cross-section. Decreases in ultimate strain and plastic energy as a function of age, an indication of the brittleness of the bone, were attributed once again to an increase in the crosslinking density of the collagen.

Conclusions

Current allograft processes alter the strength of cortical bone. The magnitude and direction of this change not only depends on the particular process but also on the direction of the applied load.

The lack of complete recovery of strength of freeze-dried bone during the reconstitution, implies either that a rehydration time of one hour (for shear) is insufficient or that the freeze drying process imparts a deleterious effect that is not compensated for through rehydration. This effect appears to be similar under the three different modes (reduction from control between 17-26%). One hypothesized cause for the latter is the induction of microfractures created by the debonding between the ceramic and the protein during the lyophilization process.

It is clear that both gamma irradiation and lyophilization independently alter the strength of cortical bone. Gamma irradiation applied while the tissue is frozen appears to increase the axial compression strength of cortical bone while weakening it under shear and transverse tension. The effect under compression appears to be dose related. A possible mechanism for this is that the irradiation process induces preferential collagen crosslinking parallel to the long axis.

Alternatively, if the irradiation is applied while the bone is in the lyophilized state and the tissue is subsequently rehydrated, the strength is similar to or slightly lower than freeze-dried and rehydrated (non-irradiated) bone. Bone in the lyophilized and irradiated state appears to be altered exclusively by the lyophilization process.

Autoclaving did not decrease the axial compression strength of cortical bone more than freeze-drying and rehydration. This may be due to the short autoclaving time (30minutes) and the fact that the specimens were well insulated in the glass vials.

Bone that is more dense fails at a higher stress. If specimens are retrieved from the denser outer cortex the strength will be greatest. This is indicated in the 1.5mm shear specimens.

The Biocleanse™ process does not alter the transverse tension or the axial compressive strength of bone.

Specimens derived from an older population of donors were found to be weaker under axial compression, shear, and transverse tension that cannot be attributed to the density of bone. Comparing the strength of this population of bone when it is in the physiologic state, it is clearly weaker. However, if this tissue is compared to a younger population of donors that has gone through some of the treatments reported here such as lyophilization and rehydration, the strength are comparable. Equivalent strengths may be obtained from this population of donors if freeze-drying and lyophilization are not performed.

This information is critical to the design process of machined allografts in order for the implant to retain biomechanical integrity, keeping patient safety and efficacy uncompromised.

CHAPTER 7 DONOR DEMOGRAPHICS, PROCESSING, AND DESIGN OF THE MD SERIES OF BONE DOWELS

Introduction

Three broad areas influence the ultimate strength of load bearing structures. These may be described as the material in which the structure is derived, the processing that the material is subjected to, and the overall design. These principles can certainly be applied within the tissue banking industry for any of the structural allografts including bone dowels.

The objective of this study was to investigate how the material, the processing, and the different designs alter the ultimate strength of bone dowels. The material was defined by the donor attributes such as age, sex, or anatomic location. Various processes were investigated including extended chemical baths, sterilization treatments such as irradiation, or preservation by lyophilization. Lastly, the differences in strength among the different dowel designs were documented.

Materials and Methods

Specimen Preparation

All specimens were manufactured by RTI's proprietary manufacturing process which included packaging in sealed bags and maintained frozen (below -20°C). All specimens that were tested met the inclusion criteria specified in chapter 3.

Donor Attributes

The specimens were retrieved from the humerus, tibia, or femur and identified as such by the processor. If the anatomic location could not be determined it was identified as unknown. All other donor information such as age, and sex was retrieved from the donor charts.

Processing Parameters

Dowels were assigned to the groups as described in Table 7-1. Control specimens were stored frozen but thawed to room temperature prior to testing. All data presented in chapter 2 was utilized as controls. Freeze-drying (FD) was performed by standard methods in a lyophilizer (Vertis Gardiner, NY) and sealed at 100-200 mTorr in a glass vial that maintained the low pressure. The irradiated specimens received between 1.5 - 2.5 Mrads (Food Technology Services, Inc Mulberry FL). The irradiated only specimens were maintained on dry ice during the entire shipping and irradiation process. Extended hydrogen peroxide treatment was performed by placing dowels in a 60ml test tube that contained at least 50ml of 3% hydrogen peroxide solution USP (Humco, Texarkana, Texas). These were placed into a sonicator filled with deionized water for 4 hours with heat that was maintained at 60°C. Extended isopropyl alcohol treatment was performed by placing dowels in a 60ml test tube that contained at least 50ml of 70% isopropyl rubbing alcohol USP (Humco, Texarkana, Texas). These were maintained at room temperature for 4 hours. Extended elevated temperature treatment was performed by placing dowels in a 60ml test tube that contained at least 50ml of 0.9% Sodium Chloride Irrigation (Baxter Healthcare Corp Deerfield, IL). The test tubes were placed in a water bath that was maintained for 4 hours at 60°C. Placing the dowels in a secure

location in the laboratory in a sealed container for 17 days performed room temperature storage treatment. Freeze-thaw cycling was performed by maintaining the dowels at -20°C for 20 hours and allowed to thaw to room temperature for 4 hours and repeated for 17 cycles. Reconstitution was performed with 0.9% NaCl in a partial vacuum for at least 1 hour prior to testing. The specimens were maintained in saline up to the time of testing.

Table 7-1 Bone dowel treatment groups

Treatment
Controls (n=101)
FD+Irr (1.5-2.5 Mrad) (n=9)
FD+Irr (1.5-2.5 Mrad)+Recon (n=20)
Frozen & irr (1.5-2.5Mrad) (n=22)
Hydrogen peroxide (n=14)
Isopropyl alcohol (n=16)
Elevated temperature (n=15)
Room temperature (n=34)
Cyclic Freeze-thaw (n=35)

Dowel Design

Differences in strength were investigated between 16mm MD-2 and 16mm MD-3 dowels as well as between 18mm MD-2 and 18mm MD-4 dowels

Experimental Design

In order to assess differences in processing conditions as well as dowel design, the study was parallel arm and designed to detect a 15% difference in strength among the different treatment groups. Significance level (α) and power ($1-\beta$) were set to 0.05 and 0.90 respectively. Under these assumptions, the specimen size for each groups was to be 17 for 16mm MD-2 dowels.

Mechanical Testing

Specimens were contained in a threaded stainless steel fixture and placed on the load cell of the MTS mechanical testing apparatus. The specimens tested as outlined in chapter 3.

Normalized Strength

The technique presented in chapter 3 was utilized to not only predict the load carrying capacity of the dowel but also combined with the destructive results to determine the normalized strength of the dowel. The strength of the dowels is defined to be the ratio of the actual failure load to the predicted failure load. Utilizing this definition of strength, a normal value for strength would be a value of 1.0; a weak dowel would be below 1.0 while a strong dowel would be above 1.0. The predicted load utilizes four variables to predict the static axial load carrying ability of the dowels. These four variables are as follows: mass, diameter mismatch, slotted endwall, and unslotted endwall. The predicted load of the 16mm MD-3 dowels was determined with the 16mm MD-2 equations while the 18mm MD-IV dowels were analyzed as if they were 18mm MD-2 dowels.

Statistical Analysis

Single factor ANOVA (Microsoft Excel) analysis was utilized to determine if any significant differences existed among the different anatomic locations. Regression analysis (Microsoft Excel) was utilized to determine if there was a dependence of age on the strength of donor age. T-test assuming unequal variances (Microsoft Excel) was utilized to determine if differences existed between the control group and each of the different process runs as well as the different designs.

Results and Discussion

Donor Demographics

Anatomic Location

Table 7-2 to 7-3 describes the normalized dowel strength for each of the anatomic locations for both 16mm MD-2 and 18mm MD-2. Statistical analysis revealed that no statistical differences could not be detected in among any of the anatomic locations ($p=0.25$ for 16mm MD-2's and $p=0.39$ for 18mm MD-2's).

Table 7-2 Variation of strength of 16mm MD-2 due to anatomic origin

Location	Normalized Strength			
	Mean	SD	Minimum	Maximum
Tibia (n=24)	0.98	0.09	0.83	1.22
Femur (n=14)	1.04	0.07	0.88	1.16
Humerus (n=36)	1.01	0.10	0.83	1.23
Unidentifiable (n=56)	1.00	0.09	0.80	1.23

Table 7-3 Variation of strength of 18mm MD-2 due to anatomic origin

Location	Normalized Strength			
	Mean	SD	Minimum	Maximum
Tibia (n=54)	0.98	0.11	0.73	1.25
Femur (n=114)	1.01	0.13	0.61	1.29
Humerus (n=20)	0.98	0.14	0.64	1.13
Unidentifiable (n=149)	1.01	0.11	0.71	1.28

Age and Sex

Tables 7-4 to 7-7 describe the normalized strength of each of the dowels as a function of donor age and sex. Regression analysis revealed a dependence of strength as a function of age. The change in strength is described by the following equations for dowels manufactured from donors between the ages of 15-80 years.

$$\sigma(\text{Actual} / \text{Predicted}) = 1.051 - 0.00129 \cdot \text{donor age}$$

Inadequate data exists to predict the strength of dowels over the age of 80 and under the age of 15. No statistical differences were identified between male and female donors.

Table 7-4 Variation of strength of 16mm MD-III as a function of donor age

Location	Normalized Strength 16mm MD-III			
	Mean	SD	Minimum	Maximum
Below 24 (n=15)	1.10	0.14	0.90	1.32
25-35 (n=11)	1.03	0.09	0.81	1.13
36-45 (n=9)	1.03	0.06	0.94	1.14
46-55 (n=20)	1.01	0.11	0.83	1.18
56-65 (n=43)	1.00	0.11	0.82	1.21
66-70 (n=16))	0.93	0.07	0.85	1.06
71-75 (n=24)	0.98	0.11	0.77	1.17
76-80 (9)	0.98	0.10	0.86	1.14
Males (126)	1.00	0.11	0.82	1.32
Females (9)	1.01	0.10	0.82	1.18

Table 7-5 Variation of strength of 16mm MD-II as a function of donor age

Location	Normalized Strength 16mm MD-II			
	Mean	SD	Minimum	Maximum
Below 24 (n=24)	1.06	0.09	0.92	1.23
25-35 (n=20)	1.01	0.07	0.83	1.09
36-45 (n=28)	0.99	0.10	0.80	1.23
46-55 (n=28)	0.99	0.10	0.81	1.20
56-65 (n=18)	0.97	0.05	0.88	1.08
66-70 (n=13)	0.99	0.10	0.88	1.12
71-75 (n=28)	0.96	0.09	0.78	1.14
76-80 (n=3)	1.02	0.04	1.02	1.05
Males (n=114)	0.99	0.09	0.78	1.23
Females (n=48)	1.00	0.10	0.79	1.23

Table 7-6 Variation of strength of 18mm MD-II as a function of donor age

Location	Normalized Strength 18mm MD-II			
	Mean	SD	Minimum	Maximum
Below 24 (n=49)	1.05	0.12	0.73	1.28
25-35 (n=39)	1.03	0.10	0.81	1.20
36-45 (n=57)	1.01	0.13	0.70	1.24
46-55 (n=87)	0.99	0.12	0.71	1.22
56-65 (n=82)	0.99	0.12	0.61	1.29
66-70 (n=17)	0.98	0.12	0.73	1.13
71-75 (n=38)	0.97	0.10	0.70	1.29
76-80 (n=14)	0.95	0.14	0.62	1.13
81-85 (n=3)	0.84	0.04	0.86	0.87
Males (n=306)	1.00	0.12	0.61	1.29
Females (n=80)	0.99	0.13	0.70	1.24

Table 7-7 Variation of strength of 20mm MD-II as a function of donor age

Location	Normalized Strength 20mm MD-II			
	Mean	SD	Minimum	Maximum
Below 24 (n=16)	1.03	0.14	0.76	1.21
25-35 (n=18)	0.96	0.16	0.55	1.22
36-45 (n=29)	0.97	0.11	0.68	1.18
46-55 (n=38)	0.96	0.12	0.62	1.14
56-65 (n=48)	0.95	0.11	0.67	1.16
66-70 (n=13)	0.96	0.11	0.68	1.10
71-75 (n=20)	0.95	0.12	0.72	1.12
76-80 (n=3)	1.01	0.10	0.90	1.09
Males (n=27)	0.94	0.16	0.55	1.18
Females (n=158)	0.97	0.11	0.62	1.22

Processing Parameters

Table 7-8 illustrates the differences in strength between typical production dowels and the various treatment groups. Statistical analysis revealed a significant difference between the control group and the following treatments freeze-drying and irradiation ($p<0.05$); freeze-dried, irradiated and rehydrated ($p<0.05$); and frozen and irradiated ($p<0.05$). Most of the 40% drop in strength in the freeze-dried and irradiated group is due to the freeze-drying process rather than the irradiation. Irradiation of dowels in the

physiologic state reduces the strength by 10% while reconstitution of freeze-dried irradiated specimens reduces the strength by 13%. The other treatments including all extended chemical baths, room temperature, and freeze-thaw cycles were found to be statistically insignificant ($p>0.05$). Differences exist between the results of bone dowels and the results from the previous chapter. This is attributed to the fact that the previous chapter applied utilized specimens that were similar in shape (cylinders of cortical bone), similar in material (density), and utilized a technique (calculated failure stress) that detect difference to better precision. In addition, the modes of loading of the cortical cylinders was pure as opposed to the bone dowels that were found (Chapter 2) to be under a complex loading scheme.

Table 7-8 Variation of strength of 16mm MD-II due to processing

	Normalized Strength 16mm MD-II			
	Mean	SD	Minimum	Maximum
Physiologic (n=101)	1.00	0.09	0.81	1.24
FD+Irr (1.5-2.5 Mrad) (n=9)	0.60	0.23	0.06	0.78
FD+Irr (1.5-2.5 Mrad)+Recon (n=20)	0.87	0.12	0.66	1.13
Frozen & irr (1.5-2.5Mrad) (n=22)	0.90	0.13	0.73	1.15
Hydrogen peroxide (n=14)	0.98	0.17	0.71	1.28
Isopropyl alcohol (n=16)	1.03	0.11	0.86	1.22
Elevated temperature (n=15)	0.93	0.13	0.74	1.15
Room temperature (n=34)	0.99	0.15	0.70	1.20
Cyclic Freeze-thaw (n=35)	0.99	0.18	0.61	1.27

Design

16mm MD-3 dowels were found to be 5% weaker than a comparable 16mm MD-2. This was found to be statistically significant ($p<0.05$). In addition, 18mm MD-4's were found to be 25% weaker than a comparable 18mm MD-2 ($p<0.05$). This is documented in Table 7-9 and 7-10.

Table 7-9 Variation in strength between 16mm MD-II and MD-III dowels

		Normalized Strength 16mm MD-II vs MD-III			
		Mean	SD	Minimum	Maximum
16mm MD-2	101	1.00	0.09	0.80	1.23
16mm MD-3	47	0.95	0.11	0.76	1.25

Table 7-10 Variation in strength between 18mm MD-II and MD-IV dowels

		Normalized Strength 16mm MD-II vs MD-III			
		Mean	SD	Minimum	Maximum
18mm MD-2	(n=259)	1.00	0.12	0.64	1.31
18mm MD-4	(n=43)	0.75	0.15	0.40	1.05

Conclusions

The strength of MD dowels does not depend on the location in which it is manufactured or the sex of the donor. However, strength was found to depend on the age of the donor.

Certain processes to which the bone is subjected to may affect the strength of the bone dowels while others do not. Irradiation degrades the strength of the dowels under axial compression.

MD-2 dowels are stronger than either MD-III or MD-IV bone dowels.

CHAPTER 8

SUMMARY

A search of the literature has shown that there is a need to be able to quantify the behavior of allografts in a structural environment. Bone can be treated as a brittle composite with a collagen polymer phase. Structural design can be optimized for mechanical behavior.

Moiré interferometry has been utilized on many different materials to observe the full deformation field. This technology has not been utilized on allograft tissue. Moiré interferometry was successfully applied on compliant cortical bone dowels in order to identify regions of high stress. The data identified similarities and differences between the *in-vivo* loading and the Hertzian loading conditions.

Previous research endeavors have attempted to correlate the load bearing capacity of allograft materials with measurable physical parameters in order to prevent *in-vivo* failures from occurring. This research identified correlations that are an improvement over documented research. A systematic method of normalizing the strength of the MD-series of bone dowels has been defined. This technique may be utilized for a variety of purposes. It may be utilized to assess differences in strength of the MD-series of bone dowels due to donor demographics, processing methodologies, and/or design.

Weibull statistics has a long history of being utilized as a quality control procedure in a variety of industries in order to prevent failures in service. The application of this technique on allograft tissue was not documented in the general literature. An

empirical treatment of failure identified by regression analysis was successfully combined with a quality criteria and Weibull analysis in order to establish a nondestructive quality control procedure in order to identify any structurally deficient dowels.

The nondestructive evaluation procedure was successfully validated. This process accurately predicts whether or not a MD-Series of dowels will survive axial compressive design loads.

Some of the changes that occur in the long bones of humans have been well documented. These changes include cortical wall thickness as a function of age and sex as well as type of bone. However, it is not known if the strength of implants that are derived from these tissues will be affected by the characteristics of the donor. The tissue banking industry has relied on many different processes in order to manufacture their final products. However, it is unclear what the role of these variables is on the strength of the final product. Lastly, different MD Dowels designs are currently being manufactured in order to maximize the strength, yield, or clinical usefulness of the dowels. Several different factors including donor demographics, processing conditions, and dowel design were explored in order to assess their effects on the strength of the bone dowels.

Current allograft processes alter the strength of cortical bone. The magnitude and direction of this change not only depends on the particular process but also on the direction of the applied load. The strength of MD dowels does not depend on the location in which it is manufactured or the sex of the donor. However, strength was found to depend on the age of the donor.

Certain processes that the bone is subjected to may affect the strength of the bone dowels while others do not. Irradiation degrades the strength of the dowels under axial compression while extended chemical treatments and room temperature storage did not.

MD-2 dowels are stronger than either MD-III or MD-IV bone dowels.

Although the proposed research has focused on the MD series of bone dowels under one mode of loading, the results of this research may be applied to other allograft products. For example, RTI has many different conventional tissue banking products such as iliac crest grafts and other specialized machine products such as SR wedges, miniscrews, bone pins, interference screws, suture anchors, to name a few, where the knowledge and results of this research may be transferred.

REFERENCES

1. American Association of Tissue Banks Standards for Tissue Banking, 1998.
2. Bioglass: What it is and how it works. Alachua, FL: US Biomaterials company brochure, 1998.
3. <http://www.cloward.com>
4. Aebi M, Regazzoni P. Bone transplantation. Berlin, New York: Springer-Verlag, p. xiii, 363, 1989.
5. Albee F. Spondylolisthesis. *J Bone Joint Surg Am* 9: 427-446, 1927.
6. Albee FH. Bone graft surgery. Philadelphia: Saunders, 1915.
7. Albee FH. Bone graft surgery in disease injury and deformity. New York: Appleton-Century, p. 403, 1940.
8. Alpert S. PMA P950002 BAK Interbody fusion system with instrumentation: summary of safety and effectiveness: Office of Device Evaluation Center for Devices and Radiological Health, 1996.
9. An HS, Simpson JM, Glover JM, Stephany J. Comparison between allograft plus demineralized bone matrix versus autograft in anterior cervical fusion. A prospective multicenter study. *Spine* 20 (20): 2211-6, 1995.
10. An HS, Xu R, Lim TH, McGrady L, Wilson C. Prediction of bone graft strength using dual-energy radiographic absorptiometry. *Spine* 19 (20): 2358-62; discussion 2362-3, 1994.
11. Anderson MJ, Keyak JH, Skinner HB. Compressive mechanical properties of human cancellous bone after gamma irradiation [published erratum appears in *J Bone Joint Surg Am* 1992 Sep;74(8):1274]. *J Bone Joint Surg Am* 74 (5): 747-52, 1992.
12. Arrington ED, Smith WJ, Chambers HG, Bucknell AL, Davino NA. Complications of iliac crest bone graft harvesting. *Clin Orthop* (329): 300-9, 1996.
13. Ashman R. Ultrasonic determination of the elastic properties of cortical bone: techniques and limitations, Tulane University, 1982.

14. Ashman RB, Cowin SC, Van Buskirk WC, Rice JC. A continuous wave technique for the measurement of the elastic properties of cortical bone. *J Biomech* 17 (5): 349-61, 1984.
15. Ashman RB, Rho JY, Turner CH. Anatomical variation of orthotropic elastic moduli of the proximal human tibia. *J Biomech* 22 (8-9): 895-900, 1989.
16. Aspenberg P, Lindqvist SB. Ethene oxide and bone induction. Controversy remains. *Acta Orthop Scand* 69 (2): 173-6, 1998.
17. Augat P, Reeb H, Claes LE. Prediction of fracture load at different skeletal sites by geometric properties of the cortical shell. *J Bone Miner Res* 11 (9): 1356-63, 1996.
18. Bailey R, Badgley C. Stabilization of the cervical spine by anterior fusion. *J Bone Joint Surg Am* 42A: 565-594, 1960.
19. Banna M. Clinical radiology of the spine and the spinal cord. Rockville, MD: Aspen Systems, p. xiv, 449, 1985.
20. Bassett C, Creighton D. A comparison of host response to cortical autografts and processed calf heterografts. *J Bone Joint Surg Am* 44a: 842-854, 1962.
21. Benzel EC. Biomechanics of spine stabilization : principles and clinical practice. New York: McGraw-Hill Health Professions Division, p. x, 278, 1995.
22. Biscogliosi A. Artificial disc to drive future spine market growth. *Orthopedics Today*. 18, 1998.
23. Bjarnason K, Hassager C, Svendsen OL, Stang H, Christiansen C. Anteroposterior and lateral spinal DXA for the assessment of vertebral body strength: comparison with hip and forearm measurement. *Osteoporos Int* 6 (1): 37-42, 1996.
24. Bloom MH, Raney FL, Jr. Anterior intervertebral fusion of the cervical spine. A technical note. *J Bone Joint Surg Am* 63 (5): 842, 1981.
25. Brantigan JW, Cunningham BW, Warden K, McAfee PC, Steffee AD. Compression strength of donor bone for posterior lumbar interbody fusion. *Spine* 18 (9): 1213-21, 1993.
26. Bridwell KH, Dewald RL. The textbook of spinal surgery. 2nd ed. Philadelphia: Lippincott-Raven, p. v. 1-567, 1997.
27. Briggs H, Milligan P. Chip fusion of the low back following exploration of the spinal canal. *J Bone Joint Surg Am* 26: 125-130, 1944.

28. Bright R. Tissue-bank standards-concerns of an orthopaedist. In: Proceeding of the American Association of Tissue Banks, 1977.
29. Burstein AH, Reilly DT, Martens M. Aging of bone tissue: mechanical properties. *J Bone Joint Surg Am* 58 (1): 82-6, 1976.
30. Bush L. The use of homogenous bone grafts. *J Bone Joint Surg Am* 29A: 620-628, 1947.
31. Buttermann GR, Glazer PA, Bradford DS. The use of bone allografts in the spine. *Clin Orthop* (324): 75-85, 1996.
32. Capener N. Spondylolisthesis. *Brit Jour Surg* 19: 374-384, 1932.
33. Carrel A. The preservation of tissues and its application in surgery. *JAMA* 59: 523-527, 1912.
34. Carson E. Doctors using pain-relieving spinal implants. *Investors Business Daily* Wednesday, March 16, 1997;A4.
35. Catanese J, Bank R, TeKoppele J, Keaveny T. Increased cross-linking by non-enzymatic glycation reduces the ductility of bone and bone collagen. In: *Proceedings of the 1999 Bioengineering Conference*, Big Sky, Montana, 1999.
36. Cheng XG, Lowet G, Boonen S, Nicholson PH, Brys P, Nijs J, Dequeker J. Assessment of the strength of proximal femur in vitro: relationship to femoral bone mineral density and femoral geometry. *Bone* 20 (3): 213-8, 1997.
37. Cloward R. The anterior approach for removal of ruptured cervical disks. *J Neurosurg* 15: 602-614, 1958.
38. Cloward R. Treatment of acute fractures and fracture-dislocations of the cervical spine by vertebral-body fusion: a report of 11 cases. *J Neurosurg* 18: 201-209, 1961.
39. Cloward R. The treatment of ruptured lumbar intervertebral disc by vertebral body fusion Part III method of use of banked bone. *Ann Surg* 136: 987-992, 1952.
40. Cloward R. The treatment of ruptured lumbar intervertebral discs by vertebral body fusion I. indications, operative technique, after care. *J. Neurosurg* 10: 154-168, 1953.
41. Cotler JM, Cotler HB. *Spinal fusion : science and technique*. New York: Springer-Verlag, p. xvi, 407, 1990.
42. Courtney AC, Hayes WC, Gibson LJ. Age-related differences in post-yield damage in human cortical bone. Experiment and model. *J Biomech* 29 (11): 1463-71, 1996.

43. Cowin S. On the strength anisotropy of bone and wood. In: Transactions of the ASME, December, 1979.
44. Cowin SC. Bone mechanics. Boca Raton, Fla.: CTC Press, p. 313, 1989.
45. Crock HV. Anterior lumbar interbody fusion: indications for its use and notes on surgical technique. Clin Orthop (165): 157-63, 1982.
46. Currey JD, Brear K, Zioupos P. The effects of ageing and changes in mineral content in degrading the toughness of human femora [published erratum appears in J Biomech 1997 Sep;30(9):1001]. J Biomech 29 (2): 257-60, 1996.
47. Dally JW, Riley WF. Experimental stress analysis. 3rd ed. New York: McGraw-Hill, p. xxii, 639, 1991.
48. de Looze MP, Visser B, Houting I, van Rooy MA, van Dieen JH, Toussaint HM. Weight and frequency effect on spinal loading in a bricklaying task. J Biomech 29 (11): 1425-33, 1996.
49. Dechow PC, Nail GA, Schwartz-Dabney CL, Ashman RB. Elastic properties of human supraorbital and mandibular bone. Am J Phys Anthropol 90 (3): 291-306, 1993.
50. Dennis S, Watkins R, Landaker S, Dillin W, Springer D. Comparison of disc space heights after anterior lumbar interbody fusion. Spine 14 (8): 876-8, 1989.
51. Deyo RA. Low-back pain. Sci Am 279 (2): 48-53, 1998.
52. Ebisch R. Who's afraid of back spasms. Sky Magazine : 34-39, 1998.
53. Enker P, Steffee AD. Interbody fusion and instrumentation. Clin Orthop (300): 90-101, 1994.
54. Evans FG, Vincentelli R. Relations of the compressive properties of human cortical bone to histological structure and calcification. J Biomech 7 (1): 1-10, 1974.
55. Eyre DR, Dickson IR, Van Ness K. Collagen cross-linking in human bone and articular cartilage. Age- related changes in the content of mature hydroxypyridinium residues. Biochem J 252 (2): 495-500, 1988.
56. Felbeck DK, Atkins A. Strength and fracture of engineering solids. 2nd ed. Upper Saddle River, NJ: Prentice Hall, p. xiv, 535, 1996.
57. Fideler BM, Vangsness CT, Jr., Moore T, Li Z, Rasheed S. Effects of gamma irradiation on the human immunodeficiency virus. A study in frozen human bone-patellar ligament-bone grafts obtained from infected cadavera. J Bone Joint Surg Am 76 (7): 1032-5, 1994.

58. Floman Y. Disorders of the lumbar spine. Rockville, Md. Tel Aviv, Israel: Aspen Publishers ;Freund Pub. House, p. xv, 996, 1990.
59. Friedlaender GE. Bone grafts. The basic science rationale for clinical applications. *J Bone Joint Surg Am* 69 (5): 786-90, 1987.
60. Friedlaender GE, Goldberg VM, American Academy of Orthopaedic Surgeons., National Institute of Arthritis and Musculoskeletal and Skin Diseases (U.S.). Bone and cartilage allografts : biology and clinical applications. Park Ridge, Ill.: American Academy of Orthopaedic Surgeons, p. xvi, 308, 1991.
61. Friedlaender GE, Mankin HJ, Sell KW, National Institute of Allergy and Infectious Diseases (U.S.), American Association of Tissue Banks. Osteochondral allografts : biology, banking, and clinical applications. 1st ed. Boston: Little Brown, p. xxi, 403, 1983.
62. Frymoyer JW. The Adult spine : principles and practice. 2nd ed. Philadelphia: Lippincott-Raven, p. 2 v. (xxviii, 2443, 142), 1997.
63. Fujimaki A, Crock HV, Bedbrook GM. The results of 150 anterior lumbar interbody fusion operations performed by two surgeons in Australia. *Clin Orthop* (165): 164-7, 1982.
64. Fung YC. Biomechanics : mechanical properties of living tissues. 2nd ed. New York: Springer-Verlag, p. xviii, 568, 1993.
65. Hamer AJ, Stockley I, Elson RA. Changes in allograft bone irradiated at different temperatures. *J Bone Joint Surg Br* 81 (2): 342-4, 1999.
66. Hamer AJ, Strachan JR, Black MM, Ibbotson C, Elson RA. A new method of comparative bone strength measurement. *J Med Eng Technol* 19 (1): 1-5, 1995.
67. Hamer AJ, Strachan JR, Black MM, Ibbotson CJ, Stockley I, Elson RA. Biochemical properties of cortical allograft bone using a new method of bone strength measurement. A comparison of fresh, fresh-frozen and irradiated bone. *J Bone Joint Surg Br* 78 (3): 363-8, 1996.
68. Han S, Medige J, Davis J, Fishkin Z, Mihalko W, Ziv I. Ultrasound velocity and broadband attenuation as predictors of load- bearing capacities of human calcanei. *Calcif Tissue Int* 60 (1): 21-5, 1997.
69. Harmon P. Anterior excission and vertebral body fusion operation for intervertebral disk syndromes of the lower lumbar sline: three to five-year results in 244 cases. *Clin Orthop* 26: 107-27, 1963.
70. Hass S. A study of the viability of bone after removal from the body. *Arch Surg* 7: 213-226, 1923.

71. Hench LL, Ethridge EC. Biomaterials : an interfacial approach. New York: Academic Press, p. xii, 385, 1982.
72. Hitchen PW, Rengachary SS, Traynelis VC. Techniques in spinal fusion and stabilization. New York Stuttgart ; New York: Thieme Medical Publishers ; G. Thieme Verlag, p. . cm., 1994.
73. Hobatho MC, Rho JY, Ashman RB. Anatomical variation of human cancellous bone mechanical properties in vitro. *Stud Health Technol Inform* 40: 157-73, 1997.
74. Hollinger J, Mcallister B. Bone and its repair. *Boceramics vol 8 : proceedings of the 8th International Symposium on Ceramics in Medicine*, Ponte Vedra, Florida, November 1995. Vol. 8 New York: Alden Press, pp. 3-10, 1995.
75. Holtzman RNN, McCormick P, Farcy J-PC. Spinal instability. New York: Springer-Verlag, p. xxiv, 529, 1993.
76. Inclan A. The use of preserved bone grafts in orthopaedic surgery. *J Bone Joint Surg Am* 24-A: 81-96, 1942.
77. Jaslow I. Intercorporeal bone graft in spinal fusion after disc removal. *Surg Gynecol Obst* 82: 215-218, 1946.
78. Kang JS, Kim NH. The biomechanical properties of deep freezing and freeze drying bones and their biomechanical changes after in-vivo allograft. *Yonsei Med J* 36 (4): 332-5, 1995.
79. Kaufman HH, Jones E. The principles of bony spinal fusion. *Neurosurgery* 24 (2): 264-70, 1989.
80. Kessler P, Keggi K. Mechanical problems of the dowel graft in anterior cervical fusion. *J Bone Joint Surg Am* 43A: 198-199, 1967.
81. Kohles SS, Vanderby R, Jr., Ashman RB, Manley PA, Markel MD, Heiner JP. Ultrasonically determined elasticity and cortical density in canine femora after hip arthroplasty. *J Biomech* 27 (2): 137-44, 1994.
82. Kreuz F, Hyatt G, Turner G, Bassett A. The preservation and clinical use of freeze-dried bone. *J Bone Joint Surg Am* 33A: 863-872, 1951.
83. Kubler N, Reuther J, Kirchner T, Priessnitz B, Sebold W. Osteoinductive, morphologic, and biomechanical properties of autolyzed, antigen-extracted, allogeneic human bone. *J Oral Maxillofac Surg* 51 (12): 1346-57, 1993.
84. Kumar A, Kozak JA, Doherty BJ, Dickson JH. Interspace distraction and graft subsidence after anterior lumbar fusion with femoral strut allograft. *Spine* 18 (16): 2393-400, 1993.

85. Kummer FJ, Chen D, Spivak JM. Optimal selection and preparation of fresh frozen corticocancellous allografts for cervical interbody spinal fusion. *Spine* 23 (21): 2295-8, 1998.
86. Langton CM, Njeh CF, Hodgskinson R, Currey JD. Prediction of mechanical properties of the human calcaneus by broadband ultrasonic attenuation. *Bone* 18 (6): 495-503, 1996.
87. Laurie SW, Kaban LB, Mulliken JB, Murray JE. Donor-site morbidity after harvesting rib and iliac bone. *Plast Reconstr Surg* 73 (6): 933-8, 1984.
88. Leung P-C. Current trends in bone grafting. Berlin ; New York: Springer-Verlag, p. x, 108, 1989.
89. Link TM, Majumdar S, Konermann W, Meier N, Lin JC, Newitt D, Ouyang X, Peters PE, Genant HK. Texture analysis of direct magnification radiographs of vertebral specimens: correlation with bone mineral density and biomechanical properties. *Acad Radiol* 4 (3): 167-76, 1997.
90. Loguidice VA, Johnson RG, Guyer RD, Stith WJ, Ohnmeiss DD, Hochschuler SH, Rashbaum RF. Anterior lumbar interbody fusion. *Spine* 13 (3): 366-9, 1988.
91. Loty B, Courpied JP, Tomeno B, Postel M, Forest M, Abelanet R. Bone allografts sterilised by irradiation. Biological properties, procurement and results of 150 massive allografts. *Int Orthop* 14 (3): 237-42, 1990.
92. Macewen W. The osteogenic factors in the development and repair of bone. *Ann Surg* 6: 289-306, 1887.
93. Maggio D, Pacifici R, Cherubini A, Simonelli G, Luchetti M, Aisa MC, Cucinotta D, Adami S, Senin U. Age-related cortical bone loss at the metacarpal. *Calcif Tissue Int* 60 (1): 94-7, 1997.
94. Martin RB, Boardman DL. The effects of collagen fiber orientation, porosity, density, and mineralization on bovine cortical bone bending properties. *J Biomech* 26 (9): 1047-54, 1993.
95. Martin RB, Ishida J. The relative effects of collagen fiber orientation, porosity, density, and mineralization on bone strength. *J Biomech* 22 (5): 419-26, 1989.
96. Martz EO, Goel VK, Pope MH, Park JB. Materials and design of spinal implants--a review. *J Biomed Mater Res* 38 (3): 267-88, 1997.
97. McCalden RW, McGeough JA, Barker MB, Court-Brown CM. Age-related changes in the tensile properties of cortical bone. The relative importance of changes in porosity, mineralization, and microstructure. *J Bone Joint Surg Am* 75 (8): 1193-205, 1993.

98. Melvin JW. Fracture mechanics of bone. *J Biomech Eng* 115 (4B): 549-54, 1993.
99. Mercer W. Spondylolisthesis. *Edinburgh M J* : 545-572, 1936.
100. Mosdal C. Cervical osteochondrosis and disc herniation. Eighteen years' use of interbody fusion by Cloward's technique in 755 cases. *Acta Neurochir* 70 (3-4): 207-25, 1984.
101. Nachemson A. The load on lumbar disks in different positions of the body. *Clin Orthop* 45: 107-22, 1966.
102. Nicholson PH, Lowet G, Cheng XG, Boonen S, van der Perre G, Dequeker J. Assessment of the strength of the proximal femur in vitro: relationship with ultrasonic measurements of the calcaneus. *Bone* 20 (3): 219-24, 1997.
103. Niu X, Ifju PG, Bianchi JR, Wallace B. A diffraction grating for compliant and porous materials. *Experimental Techniques* (in process), 1999.
104. Norman TL, Wang Z. Microdamage of human cortical bone: incidence and morphology in long bones. *Bone* 20 (4): 375-9, 1997.
105. O'Connor G. Merthiolate: a tissue preservative and antiseptic. *Am J Surg* : 563-565, 1939.
106. Orell S. Surgical bone grafting with os purum, os novum and boiled bone. *J Bone Joint Surg Am* 19A: 873-885, 1937.
107. Otero Vich JM. Anterior cervical interbody fusion with threaded cylindrical bone. *J Neurosurg* 63 (5): 750-3, 1985.
108. Ovens J, Williams H. Intervertebral spine fusion with removal of herniated intervertebral disk. *Am J Surg* 70: 24-26, 1945.
109. Oxland TR, Kohrs DW, Kuslich SD, W BG. Biomechanical Rationale. The BAK interbody fusion system: an innovative solution. Minneapolis, MN: SpineTech, Inc, 1994.
110. Patten CA, Caler WE, Carter DR. Cyclic mechanical property degradation during fatigue loading of cortical bone. *J Biomech* 29 (1): 69-79, 1996.
111. Pelker RR, Friedlaender GE. Biomechanical aspects of bone autografts and allografts. *Orthop Clin North Am* 18 (2): 235-9, 1987.
112. Pelker RR, Friedlaender GE, Markham TC. Biomechanical properties of bone allografts. *Clin Orthop* (174): 54-7, 1983.

113. Pelker RR, Friedlaender GE, Markham TC, Panjabi MM, Moen CJ. Effects of freezing and freeze-drying on the biomechanical properties of rat bone. *J Orthop Res* 1 (4): 405-11, 1984.
114. Pereira BP, Khong KS, Ng RT. The effect of storage at -70 degrees C and -150 degrees C on the torsion properties of the canine femur. *Ann Acad Med Singapore* 28 (1): 37-43, 1999.
115. Post D, Han B, Ifju P. High sensitivity moiré : experimental analysis for mechanics and materials. New York: Springer-Verlag, p. xxi, 444, 1994.
116. Prolo DJ, Rodrigo JJ. Contemporary bone graft physiology and surgery. *Clin Orthop* (200): 322-42, 1985.
117. Rao S, McKellop H, Chao D, Schildhauer TA, Gendler E, Moore TM. Biomechanical comparison of bone graft used in anterior spinal reconstruction. Freeze-dried demineralized femoral segments versus fresh fibular segments and tricortical iliac blocks in autopsy specimens. *Clin Orthop* (289): 131-5, 1993.
118. Ray R. Bone implants. *J Bone Joint Surg Am* 39A (5): 1119-1127, 1957.
119. Reilly DT, Burstein AH, Frankel VH. The elastic modulus for bone. *J Biomech* 7 (3): 271-5, 1974.
120. Reynolds F, Oliver D. Clinical evaluation of the merthiolate bone bank a preliminary report. *J Bone Joint Surg Am* 31A: 792-798, 1949.
121. Rho JY, Ashman RB, Turner CH. Young's modulus of trabecular and cortical bone material: ultrasonic and microtensile measurements. *J Biomech* 26 (2): 111-9, 1993.
122. Rho JY, Flaitz D, Swarnakar V, Acharya RS. The characterization of broadband ultrasound attenuation and fractal analysis by biomechanical properties. *Bone* 20 (5): 497-504, 1997.
123. Rho JY, Hobatho MC, Ashman RB. Relations of mechanical properties to density and CT numbers in human bone. *Med Eng Phys* 17 (5): 347-55, 1995.
124. Roark RJ, Young WC. Roark's formulas for stress and strain. 6th ed. New York: McGraw-Hill, p. xiv, 763, 1989.
125. Robinson R, Smith G. Anterolateral cervical disc removal and interbody fusion for cervical disc syndrome. *Bull Johns Hopkins Hosp* 96: 223-224, 1955.
126. Robinson R, Walker A, Ferlic D, Wiecking D. The results of anterior interbody fusion of lthe cervical spine. *J Bone Joint Surg Am* 44A: 1569-1587, 1962.

127. Sacks S. Anterior interbody fusion of the lumbar spine. Indications and results in 200 cases. *Clin Orthop* 44: 163-70, 1966.
128. Scarborough NL. Current procedures for banking allograft human bone. *Orthopedics* 15 (10): 1161-7, 1992.
129. Schermerhorn D. Bodies in motion. *Compressed air* : 20-24, 1997.
130. Schipplein O. Annual meeting of the orthopaedic reaserch society. , 1991.
131. Senn N. On the healing of aseptic bone cavities by implantation of antiseptic decalcified bone. *Am J Med Sci* : 218-243, 1889.
132. Shigley JE, Mitchell LD. Mechanical engineering design. 4th ed. New York: McGraw-Hill, p. xix, 869, 1983.
133. Shinomiya K, Okamoto A, Kamikozuru M, Furuya K, Yamaura I. An analysis of failures in primary cervical anterior spinal cord decompression and fusion. *J Spinal Disord* 6 (4): 277-88, 1993.
134. Simmons EH, Bhalla SK. Anterior cervical discectomy and fusion. A clinical and biomechanical study with eight-year follow-up. *J Bone Joint Surg Br* 51 (2): 225-37, 1969.
135. Simon SR, American Academy of Orthopaedic Surgeons. Orthopaedic basic science. [Rosemont, Ill.]: American Academy of Orthopaedic Surgeons, p. xvi, 704, 1994.
136. Smith G, RA R. The treatment of certain cervical-spine disorders by anterior removal of the intervertebral disc and interbody fusion. *J Bone Joint Surg Am* 40A: 607-624, 1958.
137. Speed K. Spondylolisthesis. *Arch Surg* 37: 175-189, 1938.
138. Speirs AD, Hotz MA, Oxland TR, Hausler R, Nolte LP. Biomechanical properties of sterilized human auditory ossicles. *J Biomech* 32 (5): 485-91, 1999.
139. Stauffer RN, Coventry MB. Anterior interbody lumbar spine fusion. Analysis of Mayo Clinic series. *J Bone Joint Surg Am* 54 (4): 756-68, 1972.
140. Suhling J. Class Notes for ME 636, Auburn University, 1992.
141. Sutterlin C, Bossons C. Evaluation and treatment of degenerative instability of spinal column: a philosophical and clinical approach. *Seminars in Spinal Surgery* 8 (4): 266-291, 1996.
142. Taheri ZE, Gueramy M. Experience with calf bone in cervical interbody spinal fusion. *J Neurosurg* 36 (1): 67-71, 1972.

143. Thoren K, Aspenberg P. Ethylene oxide sterilization impairs allograft incorporation in a conduction chamber. *Clin Orthop* (318): 259-64, 1995.
144. Tomford WW. Musculoskeletal tissue banking. New York: Raven Press, p. xiii, 240, 1993.
145. Urist MR. Surface-decalcified allogeneic bone (SDAB) implants. A preliminary report of 10 cases and 25 comparable operations with undecalcified lyophilized bone implants. *Clin Orthop* 56: 37-50, 1968.
146. Vergano D. Hot-wiring can straighten out chronic back pain. *USA Today* 1999 Monday, November 29;6D.
147. Wachtman JB. Mechanical properties of ceramics. New York: Wiley, p. xxii, 448, 1996.
148. Weaver J. Experiences in the use of homogenous (bone bank) bone. *J Bone Joint Surg Am* 31A: 778-792, 1949.
149. Weiler A, Helling HJ, Kirch U, Zirbes TK, Rehm KE. Foreign-body reaction and the course of osteolysis after polyglycolide implants for fracture fixation: experimental study in sheep. *J Bone Joint Surg Br* 78 (3): 369-76, 1996.
150. White AAd, Hirsch C. An experimental study of the immediate load bearing capacity of some commonly used iliac bone grafts. *Acta Orthop Scand* 42 (6): 482-90, 1971.
151. White AAd, Jupiter J, Southwick WO, Panjabi MM. An experimental study of the immediate load bearing capacity of three surgical constructions for anterior spine fusions. *Clin Orthop* 91: 21-8, 1973.
152. Whitecloud TS, Dunsker SB. Anterior cervical spine surgery. New York: Raven Press, p. xiii, 145, 1993.
153. Wilson P. Experiences with a bone bank. *Ann Surg* 126: 932-946, 1947.
154. Wiltberger B. The prefit dowel intervertebral body fusion as used in lumbar disc therapy. *Am J Surg* : 723-727, 1953.
155. Wimmer C, Krismer M, Gluch H, Ogon M, Stockl B. Autogenic versus allogenic bone grafts in anterior lumbar interbody fusion. *Clin Orthop* (360): 122-6, 1999.
156. Wolfenbarger L, Jr., Zhang Y, Adam BL, Sutherland V, Gates K, Brame B. A comprehensive study of physical parameters, biomechanical properties, and statistical correlations of iliac crest bone wedges used in spinal fusion surgery. II. Mechanical properties and correlation with physical parameters. *Spine* 19 (3): 284-95, 1994.

157. Wolfinbarger L, Jr., Zhang Y, Adam BL, Sutherland V, Homsi D, Brame B. A comprehensive study of physical parameters, biomechanical properties, and statistical correlations of iliac crest bone wedges used in spinal fusion surgery. I. Physical parameters and their correlations. *Spine* 19 (3): 277-83, 1994.
158. Zdeblick T. Anterior cervical discectomy and fusion using a porous hydroxyapatite bone graft substitute. *Spine* 19 (20): 2348-2357, 1994.
159. Zdeblick TA, Hughes SS, Riew KD, Bohlman HH. Failed anterior cervical discectomy and arthrodesis. Analysis and treatment of thirty-five patients. *J Bone Joint Surg Am* 79 (4): 523-32, 1997.
160. Zhang Y, Homsi D, Gates K, Oakes K, Sutherland V, Wolfinbarger L, Jr. A comprehensive study of physical parameters, biomechanical properties, and statistical correlations of iliac crest bone wedges used in spinal fusion surgery. IV. Effect of gamma irradiation on mechanical and material properties. *Spine* 19 (3): 304-8, 1994.
161. Zhang Y, Wolfinbarger L, Jr. A comprehensive study of physical parameters, biomechanical properties, and statistical correlations of iliac crest bone wedges used in spinal fusion surgery. III. Multivariable regression analysis and practical formulas for strength prediction. *Spine* 19 (3): 296-303, 1994.

APPENDIX
RAW DATA, REGRESSION, AND WEIBULL ANALYSIS

Table A-1. 16mm MD-2 Dimensions, Mass, and Failure load

Test Date	Donor #	Average Diameter	diameter mismatch	average slotted	average unslotted	mass	dowel length	failure load (N)
21-May-97	uf97e006-27-04	15.9	0.0	4.2	5.0	3.515	22.6	11732
25-Jun-97	ac97f003-08-04	15.8	0.1	4.2	6.5	4.391	19.9	15752
8-Jan-97	up96i008-13-20	15.7	0.2	3.7	4.7	3.943	20.0	14131
21-May-97	cd97e001-07-15	15.7	0.1	5.4	4.9	4.334	22.6	15512
23-Apr-97	tn97a005-14-07	15.9	0.1	4.5	5.1	3.746	21.4	13206
18-Jun-97	mi97f002-14-41	15.8	0.2	5.0	5.9	4.910	21.9	18500
3-Sep-97	la97h009-07-62	15.8	0.3	4.1	4.3	3.956	19.8	14794
28-May-97	uj97e010-27-25	15.8	0.2	4.9	4.4	3.799	19.7	14029
31-Dec-96	uj96L007-13-02	16.0	0.1	4.9	4.3	3.768	20.3	13860
7-May-97	as970191-q06	15.9	0.1	4.4	4.7	3.786	19.2	14049
22-Jan-97	uf97a003-07-18	15.9	0.0	4.6	3.2	3.226	18.6	11452
1-Oct-97	ht97h003-29-26	15.9	0.0	3.7	4.7	3.682	23.2	13625
22-Oct-97	tn97d002-13-12	15.8	0.0	4.3	5.2	3.720	21.9	13727
7-Apr-97	as970107-c32	15.8	0.0	4.5	8.0	4.180	22.1	16092
28-May-97	uf97e006-27-02	15.9	0.1	4.2	5.7	3.633	20.3	13897
23-Apr-97	ac97d005-27-12	16.0	0.1	4.2	6.0	4.749	24.8	19068
7-Apr-97	am97d004-27-03	15.9	0.0	5.1	5.7	3.795	16.5	14460
2-Apr-97	um97c005-14-42	15.7	0.2	4.8	3.8	3.632	22.8	14066
18-Dec-96	uf96i002-14-03	15.9	0.0	3.5	4.5	3.846	18.1	15008
27-Aug-97	ht97g002-13-104	15.8	0.0	5.5	4.1	4.316	20.2	16970
17-Sep-97	uf97g002-14-29	16.0	0.0	3.9	5.3	4.009	19.4	15834
7-May-97	am97d011-07-09	15.7	0.2	4.6	4.3	3.899	20.6	15517
17-Sep-97	uf97g002-12-28	15.9	0.1	4.3	5.1	3.611	17.9	14040
25-Jun-97	la97f004-50-07	15.8	0.1	5.2	5.8	4.181	19.5	16612
7-Apr-97	am97d004-27-01	15.9	0.2	5.6	5.7	3.995	20.1	15871
30-Apr-97	la97c007-13-06	16.0	0.1	3.8	5.2	4.352	19.8	17805
8-Oct-97	as970641	15.7	0.2	4.4	3.8	3.075	18.2	11795
10-Feb-97	ac97b003-07-06	15.9	0.0	3.6	4.1	3.984	20.0	16077
24-Sep-97	ic97h005-08-14	15.9	0.0	4.9	4.4	3.927	19.0	15618
31-Dec-96	uj96L007-13-01#2	16.0	0.1	5.0	7.2	3.744	19.9	14814
21-May-97	cd97e004-27-12	15.9	0.1	7.7	5.8	5.640	25.7	23592
19-Feb-97	am97b002-27-10	15.8	0.0	6.6	6.2	4.419	21.7	17781
14-May-97	as970168-qc4	15.8	0.1	4.8	6.2	4.570	19.9	18947
19-Feb-97	ut97b002-08-54	15.9	0.0	5.1	4.6	3.909	19.3	15640
1-Oct-97	uj97d008-27-47	15.9	0.0	4.5	5.2	4.029	21.8	16411
21-May-97	uf97e006-27-03	16.0	0.1	3.6	4.4	2.984	17.9	11600
18-Jun-97	um97f002-27-30	15.9	0.0	4.0	4.9	3.453	22.9	13722
30-Apr-97	la97d007-08-49	16.0	0.1	6.2	6.1	4.157	22.4	16957
9-Jul-97	la97f010-07-36	15.8	0.0	4.4	6.7	4.133	20.7	17122
22-Jan-97	uf96k004-13-07	15.9	0.0	4.8	4.5	4.108	20.0	17131

31-Dec-96	lv96K003-38-02	15.8	0.2	4.3	8.6	4.730	21.9	20544
8-Oct-97	uf97c015-38-33	16.0	0.1	5.0	4.0	3.394	20.1	13714
10-Sep-97	ht96g002-27-52	15.9	0.1	4.6	4.1	3.892	18.7	16274
8-Oct-97	as970641-q02	15.7	0.0	5.3	4.6	4.124	22.5	17180
19-Feb-97	wh97b001-13-14	15.9	0.0	5.2	5.5	4.345	24.0	18309
10-Feb-97	ai97b002-14-04	15.9	0.0	5.3	8.9	4.808	23.4	20563
29-Oct-97	bb97j005-29-20	15.9	0.0	4.3	4.4	3.900	18.3	16305
5-Mar-97	am97b014-27-13	15.9	0.0	3.8	8.6	4.814	22.9	20913
15-Oct-97	up97i002-27-83	15.9	0.1	3.7	5.1	3.600	18.7	15055
8-Jan-97	lv96j006-08-06	16.0	0.1	4.7	5.8	3.736	17.2	15578
6-Aug-97	up97g011-14-32	16.0	0.1	4.9	4.8	4.331	20.3	18669
8-Oct-97	um9h007-27-48	15.7	0.0	5.3	5.0	4.187	22.1	17789
7-Apr-97	am97c015-08-16	15.8	0.1	4.3	4.6	3.315	15.6	13698
28-May-97	wh97d002-27-76	15.9	0.1	4.1	6.2	4.204	20.7	18269
11-Jun-97	as970294-q04	15.7	0.0	4.8	5.6	4.210	21.1	18056
16-Jul-97	uf97g009-13-39	15.8	0.2	3.7	4.1	3.569	20.8	15292
26-Feb-97	tn97b006-13-04	15.9	0.1	5.0	5.0	4.192	21.9	18157
23-Apr-97	ac97d005-27-04	16.0	0.1	4.7	5.9	4.809	23.3	21381
30-Apr-97	la97d007-07-48	16.0	0.1	3.7	5.0	3.360	20.4	14138
16-Jul-97	cd97g001-07-10	15.8	0.2	6.3	6.7	4.851	22.5	21582
26-Feb-97	ai97b010-07-22	15.9	0.1	4.4	5.3	4.100	20.2	17939
19-Feb-97	ai97b005-27-01	15.9	0.1	4.5	8.3	4.870	20.7	21887
10-Feb-97	uj97a016-29-05	15.9	0.0	4.3	5.1	3.778	20.0	16212
26-Feb-97	ac97b007-27-02	15.8	0.3	4.8	4.5	4.395	23.6	19882
9-Jul-97	tn97f006-27-10	16.0	0.1	4.0	5.8	3.995	23.2	17716
18-Jun-97	tn97f003-27-03	15.9	0.1	3.9	5.5	4.533	22.3	20607
19-Mar-97	la97c002-27-34	15.8	0.2	3.7	4.6	3.311	16.3	14392
30-Apr-97	wh97d002-13-53	15.9	0.2	5.8	4.7	4.299	20.3	19313
13-Aug-97	tn97f008-49-03	15.9	0.1	4.0	4.3	3.256	18.8	13972
27-Aug-97	ac97a007-30-26	15.9	0.0	3.9	4.3	3.452	19.3	14926
28-Mar-97	tn97b002-13-07	15.9	0.1	4.9	5.6	4.242	19.2	19131
17-Apr-97	am97c015-29-03	15.7	0.2	5.9	5.5	4.417	22.6	20099
4-Jun-97	as970286-q04	15.9	0.1	4.0	5.3	4.437	23.4	20380
22-Oct-97	as970688-q03	15.8	0.1	4.1	6.0	4.016	20.8	18121
29-Jan-97	la97a006-29-08	15.9	0.0	4.5	6.6	4.324	25.9	19561
14-May-97	as970168-qc5	15.8	0.1	4.9	7.8	4.791	20.0	22154
19-Feb-97	ut97b001-13-19	15.9	0.0	5.5	5.4	4.349	23.0	19576
30-Apr-97	as970250-q05	15.7	0.1	4.4	5.2	3.531	17.7	15540
7-Apr-97	as970118-041	15.9	0.1	5.4	7.9	4.905	23.8	22876
8-Jan-97	lv96j006-08-07	15.9	0.0	4.5	5.3	3.542	17.5	15558
16-Jul-97	as970431	15.8	0.0	4.0	5.8	3.798	19.5	17120
7-May-97	as970099-q04	15.8	0.1	3.0	4.4	3.587	19.6	16366
19-Feb-97	ai97b009-30-12	15.9	0.1	4.1	7.6	4.844	23.5	23036
27-Aug-97	lv97g003-29-06	15.8	0.1	3.8	4.4	3.459	17.4	15652
30-Jul-97	up97g010-14-42	15.8	0.0	4.6	5.6	4.003	20.1	18349
8-Jan-97	wh97a001-30-05	15.8	0.1	5.6	6.0	5.106	26.3	24478
4-Jun-97	cd97e006-27-06	15.9	0.1	4.0	5.8	4.003	19.9	18669
7-Apr-97	la97c006-27-56	16.0	0.0	3.1	4.1	3.237	18.8	14460
16-Jul-97	up97g008-37-17	15.9	0.0	3.8	3.9	3.168	18.1	13994
29-Oct-97	tn97d002-14-10	15.9	0.1	5.1	5.8	4.600	20.3	21876
30-Apr-97	as970250-q04	15.7	0.0	6.0	3.6	3.412	18.7	15259
27-Aug-97	tn97f008-50-04	15.7	0.2	4.5	4.5	3.435	26.9	15962
27-Aug-97	tn97f008-50-06	15.9	0.2	4.4	4.5	3.562	17.9	16843
15-Jan-97	am97a007-30-16	15.9	0.1	5.3	4.2	3.875	18.4	18326
14-May-97	as970269-q04	15.8	0.1	5.1	3.9	3.246	17.3	14839
2-Apr-97	la97c004-13-03	15.9	0.1	4.7	6.1	3.761	18.2	17982

18-Jun-97	tn97f003-27-04	15.8	0.1	3.6	4.7	3.672	20.7	17700
18-Dec-96	uf96l004-14-32	15.9	0.0	3.9	5.1	3.973	20.7	19224
19-Mar-97	am97c006-30-14	15.8	0.3	5.5	5.8	4.625	22.5	23640
14-May-97	am97e002-08-17	15.9	0.0	4.6	3.9	4.081	18.8	21046
29-Jan-97	la97a004-13-17	15.9	0.1	5.0	4.1	3.972	19.6	20784

Table A-2. Summary statistics for 16mm MD-2

Regression Statistics									
Multiple R									0.86
R Square									0.74
Adjusted R Square									0.73
Standard Error									1510.37
Observations									101
ANOVA									
	df	SS	MS		F	Significance F			
Regression	4	632826560.7	158206640.2		69.35200645	1.77171E-27			
Residual	96	218996367	2281212.156						
Total	100	851822927.7							
	Coefficients	Standard Error	t Stat	P-value	Lower 95%	Upper 95%	Lower 95.0%	Upper 95.0%	Upper 95.0%
Intercept	-2587.86	1262.97	-2.05	0.04	-5094.84	-80.88	-5094.84	-80.88	4005.42
Mismatch	1500.59	1965.43	0.76	0.45	-2400.76	5401.94	-2400.76	5401.94	4246.67
Slotted	-161.48	235.66	-0.69	0.49	-629.27	306.30	-629.27	306.30	875.76
Unslotted	-22.66	178.50	-0.13	0.90	-376.99	331.67	-376.99	331.67	879.83
Mass	5078.13	464.74	10.93	0.00	4155.63	6000.62	4155.63	6000.62	4012.71

Table A-3. Weibull analysis for 16mm MD-2 Dowel

Donor Number	Failure Load (N)	Predicted Load (N)	Ratio:Actual/ Predicted	ln(actual/pr edicted)	n=	Psi	ln(ln((1/Psi)))
uf97e006-27-04	11732	14478	0.810	-0.210	1	0.995	-5.306
ac97f003-08-04	15752	19035	0.828	-0.189	2	0.985	-4.202
up96i008-13-20	14131	17031	0.830	-0.187	3	0.975	-3.686
cd97e001-07-15	15512	18589	0.834	-0.181	4	0.965	-3.345
tn97a005-14-07	13206	15744	0.839	-0.176	5	0.955	-3.088
mi97f002-14-41	18500	21713	0.852	-0.160	6	0.946	-2.883
la97h009-07-62	14794	17193	0.860	-0.150	7	0.936	-2.710
uj97e010-27-25	14029	16122	0.870	-0.139	8	0.926	-2.562
uj96L007-13-02	13860	15811	0.877	-0.132	9	0.916	-2.431
as970191-q06	14049	15971	0.880	-0.128	10	0.906	-2.315
uf97a003-07-18	11452	12987	0.882	-0.126	11	0.896	-2.209
ht97h003-29-26	13625	15406	0.884	-0.123	12	0.886	-2.113
tn97d002-13-12	13727	15500	0.886	-0.121	13	0.876	-2.024
as970107-o32	16092	17739	0.907	-0.097	14	0.866	-1.942
uf97e006-27-02	13897	15213	0.914	-0.090	15	0.856	-1.864
ac97d005-27-12	19068	20864	0.914	-0.090	16	0.847	-1.792
am97d004-27-03	14460	15731	0.919	-0.084	17	0.837	-1.724
um97c005-14-42	14066	15295	0.920	-0.084	18	0.827	-1.659
uf96i002-14-03	15008	16287	0.921	-0.082	19	0.817	-1.598
ht97g002-13-104	16970	18357	0.924	-0.079	20	0.807	-1.539
uf97g002-14-29	15834	17029	0.930	-0.073	21	0.797	-1.483
am97d011-07-09	15517	16681	0.930	-0.072	22	0.787	-1.430
uf97g002-12-28	14040	15091	0.930	-0.072	23	0.777	-1.378
la97f004-50-07	16612	17824	0.932	-0.070	24	0.767	-1.329
am97d004-27-01	15871	16975	0.935	-0.067	25	0.757	-1.281
la97c007-13-06	17805	18940	0.940	-0.062	26	0.748	-1.234
as970641	11795	12540	0.941	-0.061	27	0.738	-1.190
ac97b003-07-06	16077	16970	0.947	-0.054	28	0.728	-1.146
ic97h005-08-14	15618	16471	0.948	-0.053	29	0.718	-1.104
uj96L007-13-01#2	14814	15605	0.949	-0.052	30	0.708	-1.063
cd97e004-27-12	23592	24829	0.950	-0.051	31	0.698	-1.023
am97b002-27-10	17781	18654	0.953	-0.048	32	0.688	-0.984
as970168-qc4	18947	19854	0.954	-0.047	33	0.678	-0.946
uf97b002-08-54	15640	16343	0.957	-0.044	34	0.668	-0.909
uj97d008-27-47	16411	17037	0.963	-0.037	35	0.658	-0.872
uf97e006-27-03	11600	12035	0.964	-0.037	36	0.649	-0.837
um97f002-27-30	13722	14199	0.966	-0.034	37	0.639	-0.802
la97d007-08-49	16957	17541	0.967	-0.034	38	0.629	-0.768
la97f010-07-36	17122	17547	0.976	-0.025	39	0.619	-0.734
uf96k004-13-07	17131	17404	0.984	-0.016	40	0.609	-0.701
lv96K003-38-02	20544	20852	0.985	-0.015	41	0.599	-0.668
uf97c015-38-33	13714	13907	0.986	-0.014	42	0.589	-0.636
ht96g002-27-52	16274	16500	0.986	-0.014	43	0.579	-0.605
as970641-q02	17180	17403	0.987	-0.013	44	0.569	-0.574
wh97b001-13-14	18309	18520	0.989	-0.011	45	0.559	-0.543
ai97b002-14-04	20563	20779	0.990	-0.010	46	0.550	-0.513
bb97j005-29-20	16305	16423	0.993	-0.007	47	0.540	-0.483
am97b014-27-13	20913	21050	0.994	-0.007	48	0.530	-0.453
up97i002-27-83	15055	15132	0.995	-0.005	49	0.520	-0.424
lv96j006-08-06	15578	15652	0.995	-0.005	50	0.510	-0.395

up97g011-14-32	18669	18657	1.001	0.001	51	0.500	-0.367
um9h007-27-48	17789	17706	1.005	0.005	52	0.490	-0.338
am97c015-08-16	13698	13607	1.007	0.007	53	0.480	-0.310
wh97d002-27-76	18269	18117	1.008	0.008	54	0.470	-0.282
as970294-q04	18056	17889	1.009	0.009	55	0.460	-0.254
uf97g009-13-39	15292	15147	1.010	0.010	56	0.450	-0.226
tn97b006-13-04	18157	17929	1.013	0.013	57	0.441	-0.199
ac97d005-27-04	21381	21090	1.014	0.014	58	0.431	-0.172
la97d007-07-48	14138	13922	1.016	0.015	59	0.421	-0.144
cd97g001-07-10	21582	21186	1.019	0.019	60	0.411	-0.117
ai97b010-07-22	17939	17561	1.022	0.021	61	0.401	-0.090
ai97b005-27-01	21887	21379	1.024	0.023	62	0.391	-0.063
uj97a016-29-05	16212	15797	1.026	0.026	63	0.381	-0.036
ac97b007-27-02	19882	19305	1.030	0.029	64	0.371	-0.009
tn97f006-27-10	17716	17073	1.038	0.037	65	0.361	0.018
tn97f003-27-03	20607	19836	1.039	0.038	66	0.351	0.045
la97c002-27-34	14392	13832	1.040	0.040	67	0.342	0.072
wh97d002-13-53	19313	18508	1.043	0.043	68	0.332	0.099
tn97f008-49-03	13972	13353	1.046	0.045	69	0.322	0.126
ac97a007-30-26	14926	14215	1.050	0.049	70	0.312	0.153
tn97b002-13-07	19131	18185	1.052	0.051	71	0.302	0.180
am97c015-29-03	20099	19074	1.054	0.052	72	0.292	0.208
as970286-q04	20380	19336	1.054	0.053	73	0.282	0.235
as970688-q03	18121	17166	1.056	0.054	74	0.272	0.263
la97a006-29-08	19561	18502	1.057	0.056	75	0.262	0.291
as970168-qc5	22154	20932	1.058	0.057	76	0.252	0.320
ut97b001-13-19	19576	18488	1.059	0.057	77	0.243	0.348
as970250-q05	15540	14666	1.060	0.058	78	0.233	0.377
as970118-041	22876	21419	1.068	0.066	79	0.223	0.407
lv96j006-08-07	15558	14560	1.069	0.066	80	0.213	0.436
as970431	17120	15930	1.075	0.072	81	0.203	0.467
as970099-q04	16366	15193	1.077	0.074	82	0.193	0.498
ai97b009-30-12	23036	21328	1.080	0.077	83	0.183	0.529
lv97g003-29-06	15652	14414	1.086	0.082	84	0.173	0.561
up97g010-14-42	18349	16878	1.087	0.084	85	0.163	0.594
wh97a001-30-05	24478	22459	1.090	0.086	86	0.153	0.628
cd97e006-27-06	18669	17122	1.090	0.087	87	0.144	0.663
la97c006-27-56	14460	13257	1.091	0.087	88	0.134	0.699
up97g008-37-17	13994	12798	1.093	0.089	89	0.124	0.737
tn97d002-14-10	21876	19975	1.095	0.091	90	0.114	0.776
as970250-q04	15259	13697	1.114	0.108	91	0.104	0.817
tn97f008-50-04	15962	14328	1.114	0.108	92	0.094	0.860
tn97f008-50-06	16843	14996	1.123	0.116	93	0.084	0.906
am97a007-30-16	18326	16298	1.124	0.117	94	0.074	0.956
as970269-q04	14839	13143	1.129	0.121	95	0.064	1.009
la97c004-13-03	17982	15773	1.140	0.131	96	0.054	1.068
tn97f003-27-04	17700	15522	1.140	0.131	97	0.045	1.135
uf96i004-14-32	19224	16843	1.141	0.132	98	0.035	1.213
am97c006-30-14	23640	20338	1.162	0.150	99	0.025	1.308
am97e002-08-17	21046	17314	1.216	0.195	100	0.015	1.437
la97a004-13-17	20784	16833	1.235	0.211	101	0.005	1.669

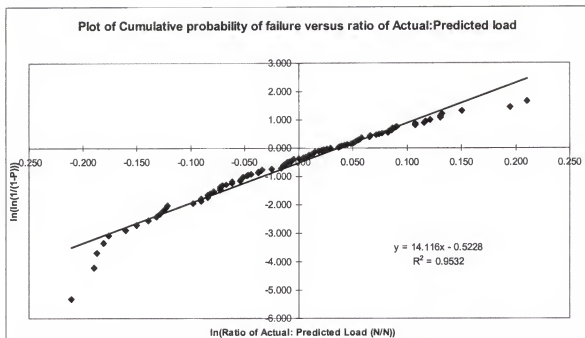



Figure A-1. Determination of Weibull modulus for 16mm MD-2

BIOGRAPHICAL SKETCH


John Bianchi was born on March 19, 1965 and is the youngest of ten children of Dr. and Mrs. Dominick Bianchi. He graduated from Bishop Kenny High School (1983) in Jacksonville, Florida. He was granted dual degrees in Bachelor of Mechanical Engineering at Georgia Tech (1988) and Bachelor of Arts at Jacksonville University (1988). After graduating, he worked at the Naval Aviation Depot as a structural Engineer. He pursued his Masters degree in Materials Science and Engineering from Auburn University (1993). His interest in spinal surgery stems from employment as a medical sales representative where he met Chester E. Sutterlin III, MD and Jamie Grooms. He is currently employed by Regeneration Technologies, Inc. He has lived a great life especially since he married his wife Laurie. They have one daughter together, Leah. Leah is hilarious.

I certify that I have read this study and that in my opinion it conforms to acceptable standards of scholarly presentation and is fully adequate, in scope and quality, as a dissertation for the degree of Doctor of Philosophy.




John J. Mecholsky, Jr., Chairman
Professor of Materials Science and
Engineering

I certify that I have read this study and that in my opinion it conforms to acceptable standards of scholarly presentation and is fully adequate, in scope and quality, as a dissertation for the degree of Doctor of Philosophy.



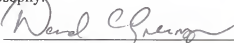
Christopher D. Batich
Professor of Materials Science and
Engineering

I certify that I have read this study and that in my opinion it conforms to acceptable standards of scholarly presentation and is fully adequate, in scope and quality, as a dissertation for the degree of Doctor of Philosophy.



Anthony B. Brennan
Associate Professor of Materials Science
and Engineering

I certify that I have read this study and that in my opinion it conforms to acceptable standards of scholarly presentation and is fully adequate, in scope and quality, as a dissertation for the degree of Doctor of Philosophy.



David C. Greenspan
Assistant Professor of Materials Science
and Engineering

I certify that I have read this study and that in my opinion it conforms to acceptable standards of scholarly presentation and is fully adequate, in scope and quality, as a dissertation for the degree of Doctor of Philosophy.



Andrew J. Rapoff

Assistant Professor of Aerospace
Engineering, Mechanics, and Engineering
Science

I certify that I have read this study and that in my opinion it conforms to acceptable standards of scholarly presentation and is fully adequate, in scope and quality, as a dissertation for the degree of Doctor of Philosophy.




Edward K. Walsh

Professor of Aerospace Engineering,
Mechanics, and Engineering Science

This dissertation was submitted to the Graduate Faculty of the College of Engineering and to the Graduate School and was accepted as partial fulfillment of the requirements for the degree of Doctor of Philosophy.

December 1999



M. J. Ohanian

Dean, College of Engineering

Winfred M. Phillips

Dean, Graduate School

LD
1780
1999
.B577

